Isotopes, Interfaces, and Geochemical Transformations

August 7-8, 2017

Geosciences Research Program, Office of Basic Energy Sciences

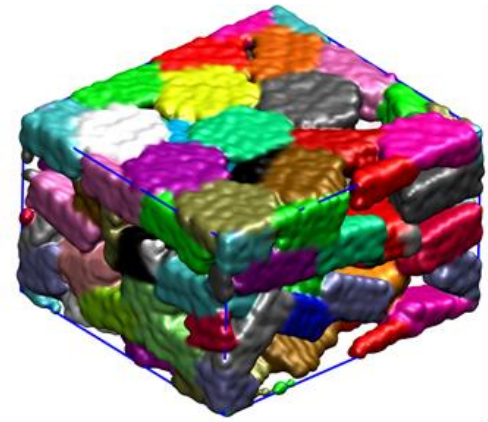

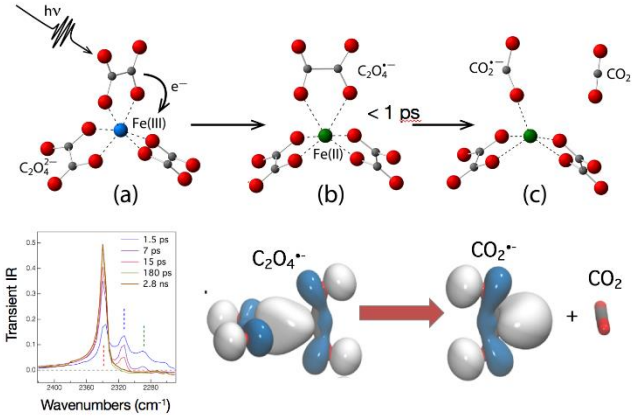

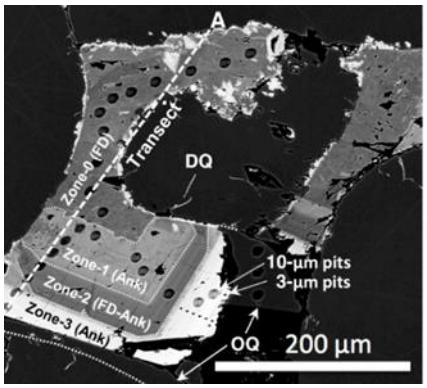

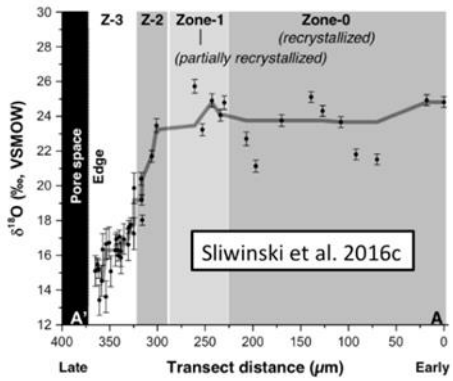

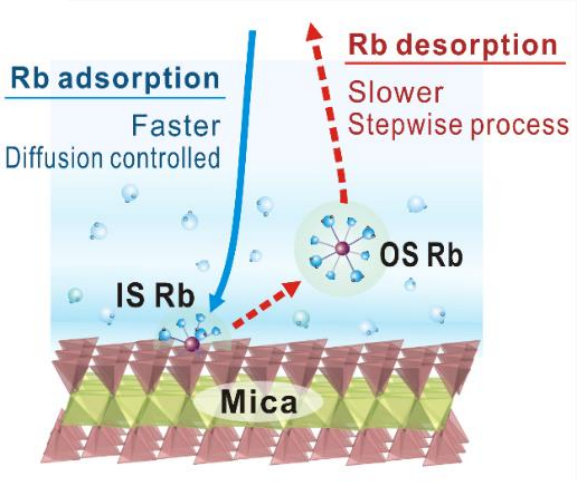

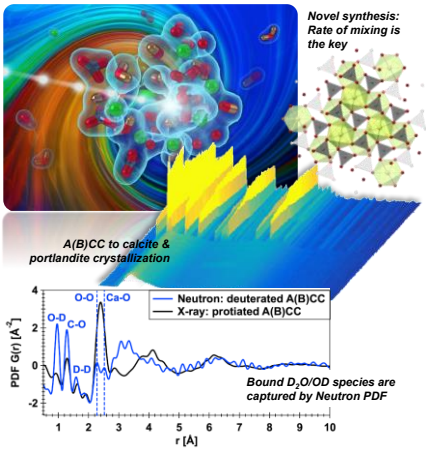

FOREWORD

"Isotopes, Interfaces, and Geochemical Transformations" is the 22nd in a series of Geosciences Research Program Symposia dating from 1995. These symposia are topically focused meetings for principal investigators in the program and provide opportunities for our investigators to give presentations on their BES-supported research. It is hoped that this meeting will provide an environment conducive to building collaborations and identifying opportunities for new research directions. In addition to seven topical sessions, this year's program has a poster session and an invited evening talk to be given by Prof. Woody Fischer of Caltech. I would like to thank this year's Session Chairs: Bill Casey (UC Davis), Ian Bourg (Princeton), Sue Brantley (Penn State), Dave Dixon (Alabama), Paul Fenter (Argonne), Mike Hochella (Virginia Tech/PNNL), and Arndt Schimmelmann (Indiana). I would also like to thank Diane Marceau of the Chemical Sciences, Geosciences, and Biosciences (CSGB) Division and Connie Lansdon of the Oak Ridge Institute for Science and Educations (ORISE) for their excellent contributions in organizing the technical and logistical aspects of this meeting.

Finally, I thank all the scientists whose vision and creativity in research and dedication and thoughtfulness in peer review have shaped the ongoing research mission of the Office of Basic Energy Sciences Geosciences Program.

Looking forward to an outstanding series of presentations.

Jim Rustad
Geosciences Research Program
Office of Basic Energy Sciences
US Department of Energy

Cover Images

Top left: Molecular-level simulation of aggregated gibbsite particles, Greathouse et al. Sandia National Laboratories.

Top right: Photo-redox generation of $C_2O_4^{\bullet-}$ and $CO_2^{\bullet-}$ in $Fe(C_2O_4)_3^{3-}$ Gilbert et al., Lawrence Berkeley National Lab and Pacific Northwest National Laboratory.

Middle: Ion microprobe transect of ^{18}O isotope variation in diagenetic carbonate cement. Valley et al., University of Wisconsin.

Bottom left: Dynamics of rubidium sorption observed with time-resolved resonant anomalous x-ray reflectivity. Lee et al., Argonne National Laboratory.

Bottom right: Neutron diffraction has been used to study the structure of amorphous calcium carbonate and its transformation to calcite, portlandite and lime. Stack et al. Oak Ridge National Laboratory.

Agenda

2017 Geosciences Program PI Meeting
U.S. Department of Energy
Office of Basic Energy Sciences
Chemical Sciences, Geosciences & Biosciences Division (CSGB)

Sunday Aug 6

4:00-6:00 pm Registration (if you miss this, you may register in the morning)
8:00-11:00 pm Informal and optional no-host reception at the Black Olive Bar & Grill (in the National Conference Center facility)

Monday Aug 7

7:00 am Breakfast

7:55 am Welcome, **Jim Rustad**, BES Geosciences Program Manager

8:00 am *BES/CSGB Update and Outlook*
Bruce Garrett, CSGB Division Director

Session 1 New Measurements in Isotope Geochemistry Bill Casey, Session Chair

8:30 am *Isotopic structures of natural organic molecules*
John Eiler, Caltech

9:00 am *Intra-molecular isotope study of light hydrocarbons*
Juske Horita, Texas Tech

9:30 am In situ *microanalysis of O & C isotope ratios in carbonate cements: SIMS standardization and preliminary data from the Bakken formation*
John Valley, University of Wisconsin

10:00 am Break

Session 2 Interfacial and Isotope Geochemistry Ian Bourg, Session Chair

10:30 am *Controls on the isotopic composition and Mg/Ca of calcite*
Don DePaolo, Lawrence Berkeley National Laboratory

11:00 am *Electrochemical kinetic isotope fractionation: theory and experiments*
Abby Kavner, UCLA

11:30 am *Clumped isotope signatures in carbonate minerals*
Aradhna Tripati, UCLA

12:00 pm Lunch

Monday Aug 7 (cont.)

Session 3 Mineral and Surface Energetics Sue Brantley, Session Chair

1:30 pm *Energetics of water, carbon dioxide, and ethanol adsorption on mineral surfaces*
Alex Navrotsky, UC Davis

2:00 pm *Calorimetric insights into mineral-water interfaces: deciphering the anatomy of an enthalpy*
Nadine Kabengi, Georgia State

2:30 pm *Ab initio thermodynamics of hydrated Mg and Ca carbonates*
Anne Chaka, Pacific Northwest National Laboratory

3:00 pm Break

Session 4

3:30 pm *Geosciences Program notes*
Jim Rustad, BES Geosciences Program Manager

4:00 pm Poster Session

6:00 pm Dinner

7:30 pm Invited Keynote Lecture

Manganese and the development of photosynthesis
Woody Fischer, Caltech

Tuesday Aug 8

7:30 am Breakfast

Session 5 Crystal Growth Dave Dixon, Session Chair

8:30 am *Particle mediated growth of iron oxides*
Jim De Yoreo, Pacific Northwest National Laboratory

9:00 am *Kinetics and thermodynamics of $CaCO_3$ nucleation in an organic matrix*
Trish Dove, Virginia Tech

9:30 am *Crystallization by particle attachment (CPA) in biominerals*
Pupa Gilbert, University of Wisconsin

10:00 Break

Tuesday Aug 8 (cont.)

Session 6 Mineral-Water Interfaces Paul Fenter, Session Chair

10:30 am *Interfacial geochemistry of nanopores: Molecular behavior in subsurface environments*
Jeff Greathouse, Sandia National Laboratory

11:00 am *Real-time observations of cation exchange at the muscovite (001) – water interface*
Sang Soo Lee, Argonne National Laboratory

11:30 am *Comparison of H_2O and Sr^{2+} positions on barite {001} studied by atomic-scale simulation and X-ray scattering*
Jim Kubicki, University of Texas, El Paso

12:00 pm Lunch

Session 7 Redox Processes Jim Rustad, Session Chair

1:30 pm *Unraveling interfacial atom and electron exchange mechanisms in Fe(II)-catalyzed iron oxide recrystallization*
Kevin Rosso, Pacific Northwest National Laboratory

2:00 pm *Kinetics of redox reactions of actinides on semiconducting minerals, as well as studtite and U_{60} clusters*
Udo Becker, University of Michigan

2:30 pm *Iron redox and photo-redox reaction mechanism from time-resolved spectroscopy*
Ben Gilbert, Lawrence Berkeley National Laboratory

3:00 pm Break

Session 8 Geochemical Transformations Arndt Schimmelmann, Session Chair

3:30 pm *Diffusion and solubility of volatiles in cryptocrystalline materials and simple oxides: CO_2 and N_2 in chert and C isotopes in polycrystalline MgO*
Bruce Watson, Rensselaer Polytechnic Institute

4:00 pm Nanoscale stress-corrosion of silicate glass in aqueous solutions
Louise Criscenti, Sandia National Laboratory

4:30 pm *Insights into geochemical transformations probed by examining solution and solid phase structures using neutron diffraction and atomic-scale simulation*
Andrew Stack, Oak Ridge National Laboratory

5:00 pm Closing, Jim Rustad, DOE/OBES

Posters

Piotrek Zarzycki, Lawrence Berkeley National Laboratory
Reactive molecular dynamics as a unique tool for understanding reactivity of mineral surfaces: Fe(II)-catalyzed recrystallization of goethite

Paul Fenter, Argonne National Laboratory
Imaging complex reactions at mineral-water interfaces

Arndt Schimmelmann, Indiana University
Genesis, storage, producibility, and natural leakage of shale gas

Sue Brantley, Pennsylvania State University
Investigating the roughness and advance rate of the weathering interface: shale, schist, diabase, granite, volcaniclastics, and serpentinite

Dave Dixon, University of Alabama
Computational studies of geochemical nanoparticles: A bottom-up approach

Bill Casey, UC Davis
An NMR probe for solution spectroscopy at geochemical pressures

Mike Hochella, Virginia Tech
New light shed on important Earth-relevant redox reactions observed at the nanoscale

Ian Bourg, Princeton
Stern layer structure and energetics at mica-water interfaces

Vitaliy Starchenko, Oak Ridge National Laboratory
Simulation of fracture dissolution in rocks: A 3D approach

Anastasia Ilgen, Sandia (Jeff Greathouse/Louise Criscenti presenting)
Adsorption of copper and iron on mesoporous alumina and silica

Yuxin Wu, Lawrence Berkeley National Laboratory

Geophysical methods for geochemical and hydrological process at mineral-water interfaces of geological media

Isotopic structures of natural organic molecules

John Eiler, Caltech

We are in a period of remarkable innovation of the technologies, methods and fields of application of measurements of isotopic contents of natural and synthetic materials. Arguably the most complex and quickly changing part of this field concerns the measurement of isotopic structures of molecules — the combination of site-specific and multiply-substituted isotopologues that contribute to their overall isotopic inventory. The most mature and widely understood approach this problem uses NMR to observe site-specific substitutions of ^{13}C and D in organic compounds. This technology is sure to develop further in technical capabilities and applied uses, but at present its limitations in sensitivity do not permit study of small samples (including many environmental, forensic or biomedical samples) or measurements of multiply substituted species. Various chemical, pyrolytic, spectroscopic and conventional mass spectrometric technologies have overcome these limitations for select isotopic properties of a few compounds (mostly simple gases), but even taken together these seem far from a truly general capability.

High-resolution mass spectrometry has a number of properties that may create such a capability, including high sensitivity and precision, applicability to a wide range of compounds with a single instrument and set of methods, and ease of integration with high-performance, automated sample preparation (e.g., GC isolation and sample introduction). We are pursuing this approach using new and experimental sector instruments (Thermo Fisher 253 Ultra and modified DFS) and a Fourier transform mass spectrometer — the Thermo Fisher Q Exactive GC, HF and Fusion. Used separately or in combination, these machines enable measurements of site-specific and clumped isotope compositions of H, C, N, O and S in diverse analytes, to precisions of ~0.1-1.0 ‰ and sample sizes down to picomols, at natural or artificially enriched isotope abundances.

We will focus on the use of these technologies to understand the natural and synthetic chemistries of amino acids — one of the few classes of organic molecules having a long history of prior experimental and theoretical studies of isotopic structure. In particular, we are examining alanine and methionine formed by or residual to biological and abiological reactions, documenting diagnostic isotopic fingerprints that could serve as the basis for new geochemical tools to characterize source substrates and environments of formation. Finally, we will discuss the expected path of future developments in this study, including the characterization of isotopic structures of amino acids from extremophilic terrestrial organisms and meteorite extracts.

Intra-Molecular Isotope Study of Light Hydrocarbons

Juske Horita

Department of Geosciences
Texas Tech University

Light hydrocarbons ($C_1 - C_{10}$) are the largest fraction of petroleum hydrocarbons. Major formation mechanisms of these light hydrocarbons include microbial, thermogenic, and abiogenic origins. It has also been increasingly recognized that hydrocarbons of varying chain-lengths can be stable even under mantle conditions and that their fluxes may play a key role in the carbon dynamics of the Earth. In the past decades, gas compositions and stable isotope ratios ($^2H/^1H$, $^{13}C/^{12}C$ or δ^2H, $\delta^{13}C$) of light hydrocarbons have been extensively utilized to investigate their origins and transport/transformation processes. Most natural compounds, including light hydrocarbons, are composed of a set of diverse isotopic molecules that differ not only in the number of isotopic substitutions, but also in the positions of isotopic substitution within a given molecule: the latter is called isotopomers, intra-molecular or position-specific isotope effects. For example, propane (C_3H_8) contains hydrogen and carbon at two energetically non-equivalent positions, methyl (CH_3-) and methylene (-CH_2-) groups. Position-specific isotope ratios can be defined as:

$$\Delta_i = \left(\frac{f_i}{F_i} - 1\right) 1000 \ \ (‰)$$

where *f* is a fraction of heavy isotopes (^2H or ^{13}C) within a given molecule that occupies the position *i* and *F* a fraction of heavy isotopes at the position *i* at random distribution. Theoretical calculations and some limited measurement data strongly support the hypothesis that the formation, transport and degradation processes of light hydrocarbons in the subsurface induce significant, perhaps unique position-specific $^{13}C/^{12}C$ and $^2H/^1H$ isotope fractionation. Thus, great potentials open up that the bulk and position-specific isotope fractionation of light hydrocarbons, in combination with theoretical/mathematical models, could provide unprecedented wealth of information on the sources, transport, and fates of light hydrocarbons in sedimentary basins and the deep Earth.

We have developed robust and routine quantitative Nuclear Magnetic Resonance (qNMR) protocols for high-precision and high-accuracy analysis of position-specific δ^2H and $\delta^{13}C$ measurements of select petroleum hydrocarbons (C_3-C_7): $1\sigma<\pm10$ and $<\pm1$‰ for Δ^2H and $\Delta^{13}C$ values, respectively. A high-pressure, light-weight NMR cell was developed for containing liquefied propane. The accuracy and precision of the ^2H and ^{13}C qNMR methods have been tested and verified for different NMR spectrometers with different ^1H-decoupling sequences, using ^{13}C-labeled compounds and an inter-laboratory comparison of a natural-abundance compound. Large amounts of natural gases have been collected in oil-gas fields with household propane tanks. A protocol has been established for separating and purifying a large amount of propane from the gases in laboratory, using a series of chemical traps and a variable-temperature cold trap. The efficiency (C_3 ≥95%) and isotopic integrity of the collection and separation method have been tested and proved with a synthetic natural gas (C_2-C_4) with known isotopic compositions of C_3.

We have been applying the qNMR method for position-specific δ^2H and $\delta^{13}C$ measurements of propane to natural gases collected from several oil-gas fields, including conventional (Permian Basin, TX) and unconventional petroleum reservoirs (Woodford shale, OK and Eagle Ford shale, TX). Our limited database show that the values of $\Delta_{2\text{-}1}=\Delta_2 - \Delta_1$, where 1 and 2 stand methyl (CH_3-) and methylene (-CH_2-) groups of propane, respectively, range widely from -190 to +40 ‰ (^2H) and -4 to +8 ‰ (^{13}C). It also appears that propane from different sources groups together. We are currently developing a general strategy for interpreting and modeling these data of position-specific isotope effects, along with other geochemical and geologic data (gas compositions, bulk isotope ratios, shale maturity).

In situ Microanalysis of O & C Isotope Ratios in Carbonate Cements: SIMS Standardization and Preliminary Data from the Bakken Fm

John W. Valley, University of Wisconsin-Madison

PROJECT OBJECTIVES (DE-FG02-93ER14389)

- Improve microanalytical techniques for *in situ* analysis of O and C isotope ratios by SIMS (ion microprobe). Develop standards for oxygen and carbon isotope analysis of mixed Ca-Mg-Fe-Mn carbonate minerals at sub-1 to 10 micron-scale by SIMS.
- Apply *in situ* stable isotope data from Bakken Fm to restrict theories of: carbonate cement genesis; conditions during cementation; controls on reservoir quality in an unconventional tight-oil system. Determine: the presence, abundance, relative timing and chemo-isotope composition of different generations of porosity-reducing carbonate cements in the Bakken Formation, ND.
- Test for the presence of isotopic zoning in the sequence of cement generations (early to late); address ideas about: continuous vs. punctuated cementation and fluid movement events; temperatures and timing of diagenesis; causes of porosity; and sources of carbonate carbon in the Bakken Fm.

Better understanding of genesis and timing of diagenetic cements contributes to larger DOE objectives, including: CO_2 sequestration in sedimentary basins, interpreting proxies of paleoclimate, underground fluid flow, water/rock interaction, and characterizing properties of oil, gas, and potable water reservoirs.

Highly precise, *in situ* analysis of stable isotope ratios is possible from 1-10 μm spots with large radius multi-collector SIMS instruments such as the IMS-1280. Accuracy, however, requires calibration standards that are chemically and crystallographically matched to samples, as no fundamental theory exists to predict instrument bias. Traditionally, carbonates have been calibrated against linear interpolations of end-member standards. We have identified homogeneous natural carbonates by analyzing ~150 samples and calibrated suites of 13 dolomite-ankerite, 11 magnesite-siderite, and 4 minor element-bearing $CaCO_3$ compositions (Sliwinski et al. 2016a,b). Instrumental bias is surprisingly non-linear. A few mol. % Fe in dolomite or calcite shifts bias by 1-2‰. Errors up to 11‰ in $\delta^{18}O$ and 5‰ in $\delta^{13}C$ result from using an Fe-free dolomite standard to analyze the Fe-bearing compositions of the dolomite-ankerite solid solution series; if linear interpolation is made between Dol and Ank standards, errors can still be over 5‰ and 2‰, respectively. Accurate analyses (±0.5‰) result from running all standards in each SIMS session followed by EPMA (WDS) for each analysis spot. These procedures open many new lines of research, in addition to diagenetic carbonate cements.

Detailed patterns of growth zoning and diagenesis can be interrogated using the new carbonate SIMS standards. We are building on work in the Illinois Basin (previous DOE funding cycle), where the Cambrian Mt. Simon sandstone aquifer is capped by mudstones of the Eau Claire Fm, which are predicted to confine 1 mega-ton of CO_2 injected by the MGSC Project in Decatur, IL. Pre-injection samples of sandstone contain multiple generations of carbonate, quartz and feldspar cements. Gradients up to 10‰/100μm in $\delta^{18}O$ record over 200 myr of burial, compaction, heating, and fluid flow. In contrast, cements in the Eau Claire are less variable and fluids were probably rock-controlled. We found no evidence for across-strike fluid flow upwards from the Mt. Simon. Knowledge of these cements will provide a baseline if future cores are drilled to study mineralization of injected CO_2 (Sliwinski et al. 2016c, 2017).

The Devonian/Mississippian Bakken Petroleum System in the Williston Basin includes major unconventional tight oil reservoirs. Early calcite cements reduce porosity in the Middle Bakken and isotopically resemble marine carbonates that have been recrystallized. Over 8 generations of later dolomite cements vary by up to 9‰/100μm in $\delta^{13}C$ with values to -9‰ likely recording the onset of organic matter maturation in adjacent shale beds. Variability of $\delta^{18}O$ is muted compared to open system cements in the Mt. Simon. The formation of these zoned dolomite cements likely enhances reservoir properties by preserving and creating porosity for storing hydrocarbons.

Aplin AC, Brodie M, Valley JW, Orland IJ, Hart BS (2017) In situ SIMS Oxygen Isotope Analyses Reveals a Continuous 300 Ma History of Carbonate Cementation and Dolomitization in the Middle Bakken. AAPG/SEG Meeting, London. Abst.

Barnes BD, Husson JM, Sliwinski MG, Denny AC, Valley JW, Peters SE (2017) Constraining the Importance of Authigenic Carbonate in the Global Carbon Cycle: A Case Study from the Bakken Fm. AAPG, Houston, Abst.

Pollington AD, Kozdon R, Anovitz LM, Georg RB, Spicuzza MJ, Valley JW (2016) Experimental calibration of silicon and oxygen isotope fractionation between quartz and water at 250ºC by in situ microanalysis of experimental products and application to natural samples. Chem. Geol. 421: 127-142.

Śliwiński MG, Kitajima, K, Kozdon, R, Spicuzza, MJ, Fournelle, JH, Valley, JW (2016a) Secondary Ion Mass Spectrometry Bias on Isotope Ratios in Dolomite-Ankerite, Part I: $\delta^{18}O$ Matrix Effects. Geostandards and Geoanalytical Res., 40: 157-172.

Śliwiński MG, Kitajima K, Kozdon R, Spicuzza MJ, Fournelle JH, Denny A, Valley JW (2016b) SIMS *bias* on isotope ratios in dolomite-ankerite, Part II: $\delta^{13}C$ matrix effects. Geostandards and Geoanalytical Res. 40: 173-184.

Śliwiński MG, Kozdon R, Kitajima K, Denny A, Valley JW (2016c) Microanalysis of carbonate cement $\delta^{18}O$ in a CO_2-storage system seal: insights into the diagenetic history of the Eau Claire Fm, Illinois Basin. AAPG Bulletin, 100: 1003-1031.

Śliwiński MG, Kitajima K, Kozdon R, Spicuzza MJ, Denny A and Valley JW (2017) In situ $\delta^{13}C$ and $\delta^{18}O$ microanalysis by SIMS: A method for characterizing the carbonate components of natural and engineered CO_2-reservoirs. International Journal of Greenhouse Gas Control, 57: 116-133.

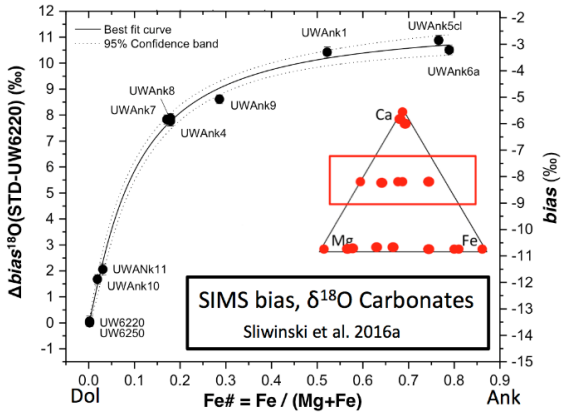

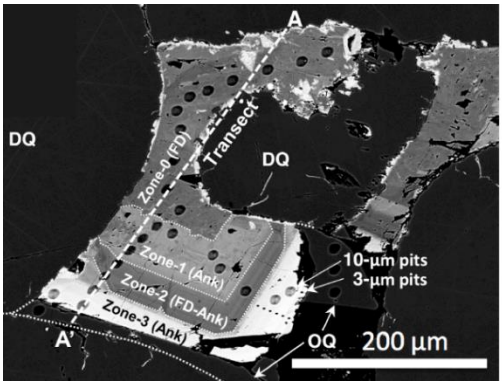

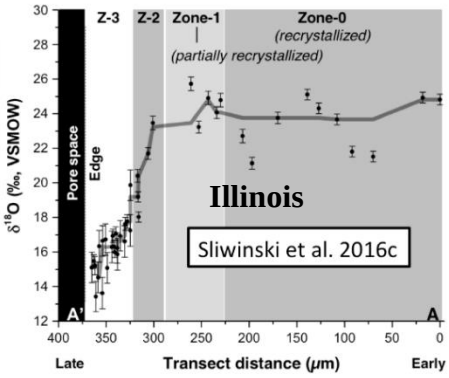

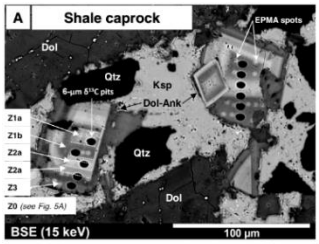

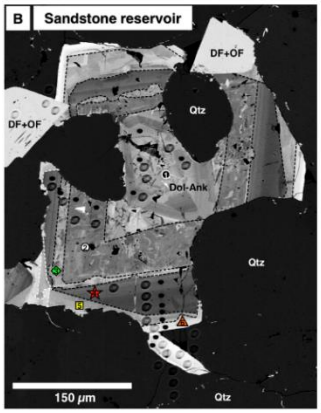

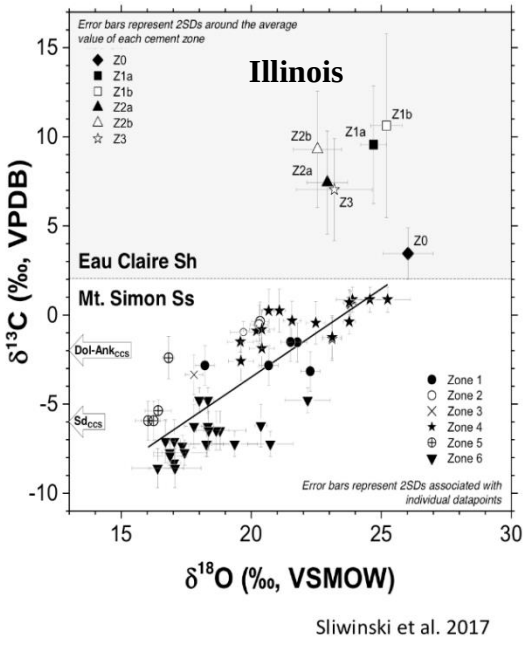

Sliwinski et al. 2017

Controls on the isotopic composition and Mg/Ca of calcite

Donald J. DePaolo, John N. Christensen, Laura Lammers, Mark Conrad, Karol Kulasinski, Shaun Brown; Lawrence Berkeley National Laboratory, University of California Berkeley

General project objectives are to understand molecular to micro-scale processes that control isotopic fractionation and trace element partitioning during mineral precipitation and transport in fluid phases. Fractionation effects are used as probes of dynamical processes in fluids and at the mineral-fluid interface, and the thermodynamics of solid solutions at low temperature. Research is based on controlled precipitation experiments, mostly on carbonates, MD simulations to identify rate-limiting processes, and measurements of natural systems to access special crystal growth conditions, laboratory inaccessible time and length scales, and systems that are likely to be in equilibrium.

In the 2011-2014 time frame we developed and published a set of models that quantitatively treat kinetic isotope (Ca, O) and trace element (Sr) effects in calcite growing from aqueous solution. This work represents the first attempt to move beyond the assumption of equilibrium isotope partitioning during calcite growth, and shows how the isotopic composition of calcite is sensitive to growth rate, pH, growth mechanism, aqueous Ca^{2+}/CO_3^{2-}, and the extent of equilibration between aqueous carbonate ions in solution. In recent work we have extended these models to encompass carbon isotopes and clumped isotopes, and begun other investigations aimed at defining the effects of aqueous Mg on Ca isotope fractionation, and understanding how isotopic fractionation is controlled during desolvation and adsorption at mineral-fluid interfaces. Deep-sea carbonate sediments and pore fluids are used to assess equilibrium Mg/Ca and Sr/Ca partitioning and the thermodynamic drivers of ultra-slow dissolution-precipitation over millions of years.

Although there are still essential data needs to test models, ion-by-ion calcite growth models have been extended to include carbon isotopes, making it possible to treat clumped C-O isotopes. These models suggest that kinetic effects on clumped isotopes are relatively small but systematic. Colleagues have extended the models to include the extent of disequilibrium in calcite O isotopes due to isotopic disequilibrium among dissolved carbonate species. Further insights into the causes of kinetic isotope fractionation during calcite growth are derived from molecular simulations, using metadynamics and umbrella sampling calculations to determine the free energy profile of Ca^{2+} ions attaching to a calcite growth site. The rate-limiting step for precipitation, which should also control isotopic fractionation, is the transition from inner-sphere complex to kink site, which involves removal of ≈1.7 coordinating water molecules. Study of natural calcite and aragonite precipitation associated with alkaline springs in an ultramafic complex in northern California, shows that while the carbonates show extreme fractionations of C and O isotopes, Ca isotope fractionation responds only to growth rate and fits existing models for α_{precip}. Study of secondary carbonate in ODP Site 807 core indicates that the equilibrium $K_{Mg/Ca}$ for calcite varies strongly with temperature from ~ 0.01 at 25°C to 0.002 at ~10°C in seawater, consistent with inferences based on growth T in foraminifera. The result requires that the activity coefficient of the Mg component in calcite solid solution have an exceptionally strong T-dependence at T < 25°C. Deep-sea carbonate pore fluids also indicate that the equilibrium $K_{Sr/Ca}$ for calcite at T < 15°C is close to 0.025, consistent with experimental data at equivalent pH and slow growth rates.

Electrochemical kinetic isotope fractionation: theory and experiments

Abby Kavner
UCLA

Stable isotopes are a sensitive marker for kinetic processes of electrochemical reactions in solutions and at solid/liquid interfaces. The goal of this research program is to develop predictive frameworks to understand local chemical reaction processes occurring at reactive interfaces, especially electrochemically active interfaces. This information will help to optimize isotope fractionation techniques, develop methods to use isotopes to characterize the energetics of chemical reactions at electrochemical surfaces, and to inform interpretation of observed isotope abundances in natural environments in terms of their generative processes. Here we summarize our body of previous experimental studies demonstrating larger-than-equilibrium and rate-dependent stable isotope fractionations during electroplating of Li, Zn, and Fe. The interplay between mass-transport and redox kinetics suggest that larger isotope fractionations occur close to the electrified interface, and compete with smaller isotope fractionations associated with the kinetics of mass transport in the solution. We introduce a newly-developed framework based on Marcus electrochemical kinetics that predicts the rate- and temperature- dependent kinetic isotope effects associated with electrochemical processes. This framework is used to make a series of quantitative predictions of the kinetic isotope effect for three specific systems: Fe^{+2}-Fe^{+3} aqueous redox exchange experiments, lithium metal electrodeposition, and mercury redox processes. We present our proposed experimental approaches to test the hypotheses.

Clumped Isotope Signatures in Carbonate Minerals

Aradhna Tripati

Carbonate 'clumped isotope' thermometry is a powerful emerging isotopic tool being applied to both inorganic and biological precipitates to probe the temperature history and fluid composition of surface and subsurface environments. It is based on measurements of the abundance of ^{13}C and ^{18}O isotopes that are bound to each other with carbonate minerals. The quantity of ^{13}C-^{18}O bonds (so-called heavy isotope 'clumps') is controlled by the physiochemical parameters of the solution at the time of mineral precipitation. Carbonate clumped isotope thermometry assumes the *attainment of internal bulk thermodynamic equilibrium* among isotopologues within a carbonate mineral. If equilibrium is reached, then ^{13}C-^{18}O bond abundance can be used to measure the temperature of precipitation without characterizing the isotopic composition of coeval fluids, a significant advantage over other widely utilized oxygen-isotope or elemental-ratio temperature proxies.

The goal of this work is to build a solid framework from which to interpret clumped isotopic signatures in geological samples from a variety of conditions, which would improve applications to study processes as wide-ranging as carbonate biomineralization and diagenesis. This talk will give an overview of our recent results and planned work that is addressing several major knowledge gaps in carbonate clumped isotope geochemistry within the analytical, experimental, and theoretical realms. These range from fundamental questions about thermodynamic and kinetic controls on clumped isotope fractionations, to the nature of potential biases introduced from sample preparation, digestion, and analysis.

Energetics of water, carbon dioxide, and ethanol adsorption on mineral surfaces

Alexandra Navrotsky and Lili Wu
Peter A. Rock Thermochemistry Laboratory and NEAT ORU
UC Davis
Davis CA 95616

Using gas adsorption calorimetry at room temperature, the enthalpies of adsorption of water, carbon dioxide, and ethanol vapor on the surfaces of amorphous silica, TiO_2 anatase and rutile, gamma alumina, and calcite have been measured. Water adsorption generally follows Langmuir isotherms, with gradual decrease on the magnitude of the exothermic adsorption energy with increasing coverage. As anticipated, materials with higher surface energies show more exothermic adsorption enthalpies. The energetics of the first few doses is consistent with dissociative adsorption, while at high coverage, the enthalpy of condensation of water vapor is approached. The behavior of ethanol is much more complex, showing several stages of adsorption and plateaus in the energetics. There is evidence of structuring of ethanol on the surface (hydrophilic end bonding to the mineral surface) which results in diminished bonding in the first few layers of ethanol. The initially strongly bound water and ethanol is difficult to remove under normal degas conditions at ambient temperature. CO_2 generally bonds more weakly than H_2O or EtOH. Implications for geochemical and biological processes are discussed.

Calorimetric insights into mineral-water interfaces: deciphering the anatomy of an enthalpy

Nadine Kabengi.
Department of Geosciences and Department of Chemistry
Georgia State University, Atlanta, GA 30302

Program Scope

The overarching goal of this project is to complete a systematic study of the thermodynamics properties of interfacial reactions across metal oxides oxides and ions/ligands of various characteristics through the application and construction of unique and specialized flow adsorption microcalorimetry techniques and instrumentations. The overall research goal will be accomplished by completing the following three specific objectives (O): O1) Determine the energetics of surface protonation and deprotonation, ion exchange and ligand sorption reactions; O2) Investigate the surface charge thermodynamic properties under a range of temperature and solution chemical compositions; and O3) Develop predictive trends of the interplay between MO structure, surface coverage and surface reactivity. In addition to key thermodynamics parameters, calorimetric measurements provide a wealth of mechanistic information about reactions energetics and kinetics, surface charge characteristics, and structure-reactivity or selectivity relationships, all obtained in-situ and in real-time. The data obtained will bridge theoretical computational predictive approaches with macroscopic analytical phenomena to yield vastly improved models of the mineral-aqueous solution and other fluid-solid interfacial phenomena.

Research Highlights

We have investigated the energetics of alkali and alkali earth cation adsorption and exchange at the rutile-water and quartz-water interface. For rutile, the thermodynamics data were rationalized with the aid of a molecularly-constrained surface complexation model (SCM) which incorporated the inner-sphere binding observed experimentally for the cations on the rutile (110) surface. Explicitly accounting for i) inner-sphere binding and ii) surface charge differences resulted in heat of exchange ratios which agreed very well (to within 0.1) with those measured. In the quartz study, the experimental thermodynamic data were analyzed to investigate chemical trends in adsorption and exchange through calculated correlations to relevant cation specific properties. Results showed that ion adsorption or exchange reactions implicate processes involving their hydration shell, and suggest inner-sphere adsorption for all the cations studied. Combined with recent X-ray reflectivity and computational reports on cations binding on quartz and muscovite reviewed above, our experimental data extends the evidence for inner-sphere complexation to all alkali and alkali earth cations and shed light on interesting kinetic differences. In both cases, we documented the role ΔH_{hyd} plays in rationalizing cation exchange reactions and controlling their net overall enthalpic sign. The consistency of this finding across solids, if proven to hold in future studies, is exciting as it may indicate the prominent role the “aqueous side” of the interface plays in controlling the energetics of interfacial reactions. This may lead to a much needed simplification of the complexity that exists across the “solid side” of the interface, which would simplify modelling efforts.

Publications

1. *Situm, A*.; *Rahman*, M.A.; *Allen*, N.; Kabengi, N.; Al-Abadleh, H. ATR-FTIR and flow microcalorimetry studies on the initial binding kinetics of arsenicals at the organic-hematite interface. *J. Phys. Chem. A.* 2017. In press. *(IF=2.883)*

2. *Allen, N.;* Machesky, M.; Wesolowski, D.; Kabengi, N. Calorimetric study of alkali and alkaline earth cation adsorption and exchange at the quartz-solution interface. *J. Colloid Interface Sci.* 2017. 504, 538-548. *(IF=3.782)*

3. *Hawkins, T.*, *Allen, N*., Machesky, M., Wesolowski, D., Kabengi, N. Ion exchange thermodynamics at the rutile-water interface: flow microcalorimetric measurements and surface complexation modeling of Na-K-Rb-Cl-NO3 adsorption. *Langmuir*. 2017, 33(20), 4934-4941. *(IF=3.993)*

Ab initio thermodynamics of hydrated Mg and Ca carbonates

Anne Chaka, Pacific Northwest National Laboratory

Ca and Mg carbonates and hydrates are important for a wide variety of concerns such as carbon sequestration, paleo environmental indicators, biomineralization, remediation, scale formation, concrete, and cement. Their formation and transformation depend upon environmental conditions, but the pathways are not well understood, nor is how what is learned in an aqueous environment transfers to CO_2-rich conditions. *Ab initio* thermodynamics based on density-functional theory with dispersion and heat of formation correction schemes linked to experimental chemical potentials for H_2O-rich and CO_2-rich systems is used to determine the stability of magnesium and calcium carbonate polymorphs as a function of environmental conditions. Understanding how Mg and Ca carbonate coordination and energies change successively from the fully hydrated structures to the minimally and fully dehydrated stages provides insight into the underlying mechanisms of carbonate formation. Ostwald's Rule of Stages is a useful approximation to understand the crystallization process, but insufficient. Key factors are the relationship between the structure of ion pairs in solution and in the crystal, as well as the availability of water diffusion pathways for dehydration. AIT calculations show that 1) in water-saturated supercritical CO_2 nonclassical low energy pathways are available for calcite formation, 2) Mg incorporation into hydrated Ca carbonate polymorphs increases water-binding energies and can stabilize the hydrated polymorphs at high Mg chemical potential, and 3) Structural distortions and thermodynamics determine why Mg-analogues of the Ca carbonate mono- and hexahydrate minerals do not form, and vice versa.

Particle Mediated Growth of Iron Oxides

Guomin Zhu, Xin Zhang, Jennifer Soltis, Sebastien Kerisit, Maria Sushko, Zhizhang Shen, Eugene Ilton, Chris Mundy, Kevin Rosso and Jim De Yoreo

Physical Sciences Division, Pacific Northwest National Laboratory, Richland, WA 99352

Growth of single crystals through assembly of primary nanoparticles appears to be a common phenomenon in geochemical, biological and synthetic settings, but assembly pathways are diverse and no quantitative framework exists for predicting their progression. In some systems, growth involves oriented attachment, a process by which the primary nanocrystals rotate into crystallographic alignment before attaching. However, in others, particle aggregation occurs with poor or random alignment and is followed by an unknown coarsening process that lead to eventual alignment of the lattice planes. In many cases, the primary particles constitute a distinct phase, which is often poorly ordered and stable only at small size and converts to the bulk phase at some point during or after assembly. For example, ferrihydrite (Fhy) commonly serves as a primary phase for particle-based growth of more ordered iron oxide phases such as hematite (Hm) and goethite (Gt). In this research, we address the challenge of developing a predictive framework for particle-based mineral growth by combining imaging of assembly processes and products, and measurements and simulations of both solution structure and inter-particle forces for a number of mineral systems, with a particular focus on iron oxides. TEM analyses of Hm crystals formed from primary Fhy nanoparticles show that the first Hm particles form by heterogeneous nucleation on or direct conversion of the Fhy particles. Growth then proceeds by preferred attachment along the (001) crystallographic axis of Hm to create a porous spindle-shaped single crystal with an internal rod-like substructure. However, while some Fhy particles can be found at the surface of the spindles, nearly all attached particles consist of Hm, many of which are misaligned. Aging leads to local faceting and co-alignment. The data demonstrate that the dominant crystallization pathway is either Fhy attachment followed by rapid conversion to oriented Hm, or formation of new Hm particles near the interface of the existing Hm at the expense of nearby Fhy particles. Using oriented single-crystal AFM tips fabricated via a focused ion beam, we also investigated crystal-crystal interaction forces in a solvent separated state for TiO_2, muscovite, and ZnO. The data show clear orientation dependencies exhibiting the symmetry of the crystal lattice. While molecular dynamics simulations predict such dependencies, the typical nm inter-particle separations over which they are predicted to be manifest are difficult to reconcile with the larger minimum separation distances estimated in the experiments. In contrast, calculations of van der Waals forces indicate orientation dependencies at distances well beyond a nm can arise from anisotropies in the dielectric constants of minerals. These findings, combined with observations in other, chemically distinct systems, reveal the importance of local chemical environments created by solid-solution interfaces in driving formation of particles that assemble to form a final crystal, as well as the importance of dispersion forces in driving co-alignment in the solvent separated state.

Kinetics and Thermodynamics of $CaCO_3$ Nucleation within an Organic Matrix

Patricia Dove (dove@vt.edu), Nizhou Han, Sebastian Mergelsberg
Department of Geosciences
Virginia Tech

High-resolution images show field and laboratory minerals from biological and geological settings form by alternate, nonclassical pathways. These include the aggregation of nanoparticles, oriented attachment of fully formed crystals, and sequential nucleation and transformation processes to form multi-layer composites. Recent findings from our studies of crystal nucleation are contributing to this multidisciplinary effort to modernize traditional paradigms of how crystals grow in aqueous solutions. Examples from this DOE project include nucleation onto functionalized polysaccharides (Giuffre et al., 2013; Giuffre et al., in prep.) and SAMS (Hamm et al., 2014), isotope tracer signatures (Giuffre et al., 2016), and calcification via amorphous calcium carbonate (ACC) (Blue et al., 2013, 2015, 2017)

Most studies of mineral nucleation, by our group and others, have investigated nucleation onto substrates immersed in bulk solutions. This approach has greatly informed our understanding of how functional group chemistry regulates energy barriers to nucleation. However, the *in vivo* formation of biominerals occurs within an organic assemblage of macromolecules. This 'organic matrix' can be localized within a compartment, at a membrane-matrix interface or within a specialized vesicle or intercellular compartment with one or more ions actively (pumped) or passively (diffused) supplied to the site of mineralization. Good examples are found in the polysaccharides of stromatolites or the protein-dominated assemblages of corals and mollusks.

In a step toward understanding how an organic matrix directs calcium carbonate biomineralization within a macromolecular environment, we developed an experimental method to measure $CaCO_3$ nucleation rate on/within a membrane of finite thickness. The approach uses a double flow-through design whereby the reagents are separated by a characterized organic film that simulates a simple tissue; we measure the kinetics and energy barrier to nucleation. Our approach combines insights from previous studies of crystal formation within hydrogels with observations from biological studies and efforts to investigate mineral nucleation within synthetic vesicles.

As proof of concept, we determined the rates and energy barriers to $CaCO_3$ nucleation for a series of proteinaceous membranes. Each gelatin was prepared by pretreating to present three types of charged functional group chemistries: 1) carboxyl and amine groups are available (non-cross linked, control); 2) carboxyl groups available (amine groups blocked by treatment with glutaraldehyde); 3) no charged groups available (carboxyl and amine groups blocked by EDC).

Preliminary measurements determine the rate of calcite nucleation decreases with increasing membrane thickness as expected. However, the thermodynamic barrier to nucleation is independent of membrane thickness (α_{cal} = 79±5 mJ/m^2) and in good agreement with nucleation onto carboxylated SAMs (Nielsen et al., 2012; Hamm et al., 2014). By tuning reagent chemistry, we produce aragonite and determine a higher energy barrier (α_{arag} = 98±10 mJ/m^2). Although reliable α_{arag} are not available, the relative magnitudes ($\alpha_{cal} < \alpha_{arag}$) are consistent with theoretical estimates (Sun, 2015, *PNAS*). The model membrane approach to measuring nucleation rates holds promise for understanding the physical basis for mineralization within intercellular or extracellular organic matrix environments.

Crystallization by particle attachment (CPA) in biominerals.

Pupa Gilbert, University of Wisconsin-Madison

Crystallization done by living organisms, termed biomineralization, involves biological control over crystal nucleation, growth, and crystal orientation patterns in the final biomineral. Marine biomineralization mechanisms are only beginning to be understood, are often surprising, and important to understand fossils and early life, to explain isotopic signatures, and to predict the fate of biomineralizers in warming, acidifying oceans.

Here I will describe one possible mechanism of crystallization by particle attachment (CPA) [1], which we recently observed in fresh, forming coral skeletons [2], and had previously observed in mollusk shell nacre [3], in sea urchin spicules [4,5] and teeth [6]. Before attaching, the particles are amorphous [2], they remain amorphous after attachment, when they completely fill three-dimensional space [7]. Finally crystallinity percolates through the amorphous solid, at the expense of the amorphous precursors, as it random-walks in three-dimensions. Proteins are occluded and slightly disorder the final crystalline biomineral [8].

Methods I developed for this research include:

1. Component mapping, which display with colors the spatial distribution of the amorphous precursors in forming, fresh biominerals [2-4].
2. Polarization-dependent Imaging Contrast (PIC)-mapping, which displays in colors the patterns of crystal orientations [9], varying wildly from the nano- to the micro-scale in marine biominerals [10-12]. PIC-maps also revealed that the physical structure of nacre correlates with the environmental temperature at the time of formation [11].

[1] J. J. De Yoreo *et al.*, Science **349**, aaa6760 (2015).
[2] T. Mass *et al.*, Procs Natl Acad Sci **accepted for publication** (2017).
[3] R. T. DeVol, C.-Y. Sun, M. A. Marcus, S. N. Coppersmith, S. C. B. Myneni, and P. U. P. A. Gilbert, J Am Chem Soc **137**, 13325 (2015).
[4] Y. U. T. Gong, C. E. Killian, I. C. Olson, N. P. Appathurai, A. L. Amasino, M. C. Martin, L. J. Holt, F. H. Wilt, and P. U. P. A. Gilbert, Proc Natl Acad Sci USA **109**, 6088 (2012).
[5] Y. Politi, R. A. Metzler, M. Abrecht, B. Gilbert, F. H. Wilt, I. Sagi, L. Addadi, S. Weiner, and P. U. P. A. Gilbert, Procs Natl Acad Sci USA **105**, 17362 (2008).
[6] C. E. Killian *et al.*, J Am Chem Soc **131**, 18404 (2009).
[7] L. Yang, C. E. Killian, M. Kunz, N. Tamura, and P. U. P. A. Gilbert, RSC-Nanoscale **3**, 603 (2011).
[8] R. A. Metzler, G. A. Tribello, M. Parrinello, and P. U. P. A. Gilbert, J Am Chem Soc **132**, 11585 (2010).
[9] P. U. P. A. Gilbert, A. Young, and S. N. Coppersmith, Proc Natl Acad Sci USA **108**, 11350 (2011).
[10] C.-Y. Sun, M. A. Marcus, M. J. Frazier, A. J. Giuffre, T. Mass, and P. U. Gilbert, ACS Nano **11**, 6612 (2017).
[11] P. U. P. A. Gilbert *et al.*, Earth and Planetary Science Letters **460**, 281 (2017).
[12] B. Pokroy, L. Kabalah-Amitai, I. Polishchuk, R. T. DeVol, A. Z. Blonsky, C.-Y. Sun, M. A. Marcus, A. Scholl, and P. U. P. A. Gilbert, Chem Mater **27**, 6516 (2015. JOURNAL COVER.).

Interfacial Geochemistry of Nanopores: Molecular Behavior in Subsurface Environments

Jeffery A. Greathouse[1], Louise J. Criscenti[1], Anastasia G. Ilgen[1], and Kevin Leung[2]

[1]Geochemistry Department and [2]Nanostructure Physics Department
Sandia National Laboratories, Albuquerque, New Mexico 87185

The goal of our project is to provide a molecular-level understanding of interfacial geochemistry within nano-scale pores. Such pores are widespread in geological systems (e.g., mudrocks), and are characterized by large surface areas and structured interfacial solutions that in combination result in different geochemical properties than those found in ideal bulk water-mineral systems. We combine both computational and experimental expertise to focus on two research tasks: Chemistry under Nano-Scale Confinement, and Upscaling from the Nano- to the Meso-Scale.

Results will be presented to highlight our recent efforts to investigate nano-scale processes. Experiments on the adsorption of aqueous ions in mesoporous silica and alumina with fixed pore sizes ranging from 2 to 8 nm are used to quantify the impact of ionic radii and hydration energies on ion adsorption under nano-scale confinement. Initial results indicate a pore size effect for copper (Cu^{2+}) adsorption on mesoporous silica, specifically increased Cu^{2+} adsorption in 4-nm pores compared with 6- and 8-nm pores. Accompanying *ab initio* molecular dynamics (AIMD) simulations provide details of the energetics and local ion coordination environments as ions adsorb to silica surfaces. Recent results indicate that divalent cations (Mg^{2+}, Cu^{2+}) adsorb at deprotonated silanol sites on the silica surface more strongly than monovalent cations (Na^{+}).

We have also developed a new method for creating nano- and mesoporous molecular models based on nanoparticle aggregates (see figure on following page). Physical properties such as surface area, porosity, and water content depend on the conditions chosen for compaction and dewatering. These novel porous mineral aggregates will be used to as a representative REV to simulate the impact of interfacial properties in a heterogeneous porous system more analogous to those found in natural geological systems compared to the highly symmetric and idealized pores traditionally used in simulation studies.

Simulations of interfacial properties in realistic pore geometries require additional development and validation of classical force field models that incorporate the range of surface terminations (particularly hydroxyl groups) expected at mineral surfaces. The development of improved edge-site models within our classical force field approach applied to clay minerals and other layered structures (ClayFF) greatly expands our simulation capability from basal surfaces to reactive edges. We have developed additional parameters to model M-O-H hydroxyl groups (M = Al, Mg, Si) common to surfaces and edges in a variety of mineral environments. Simulated structural and vibrational properties are validated by comparison with quantum calculation. Additionally, vibrational properties of deuterated edge hydroxyl groups of a clay mineral endmember (pyrophyllite) have been simulated for comparison with corresponding experimental spectra.

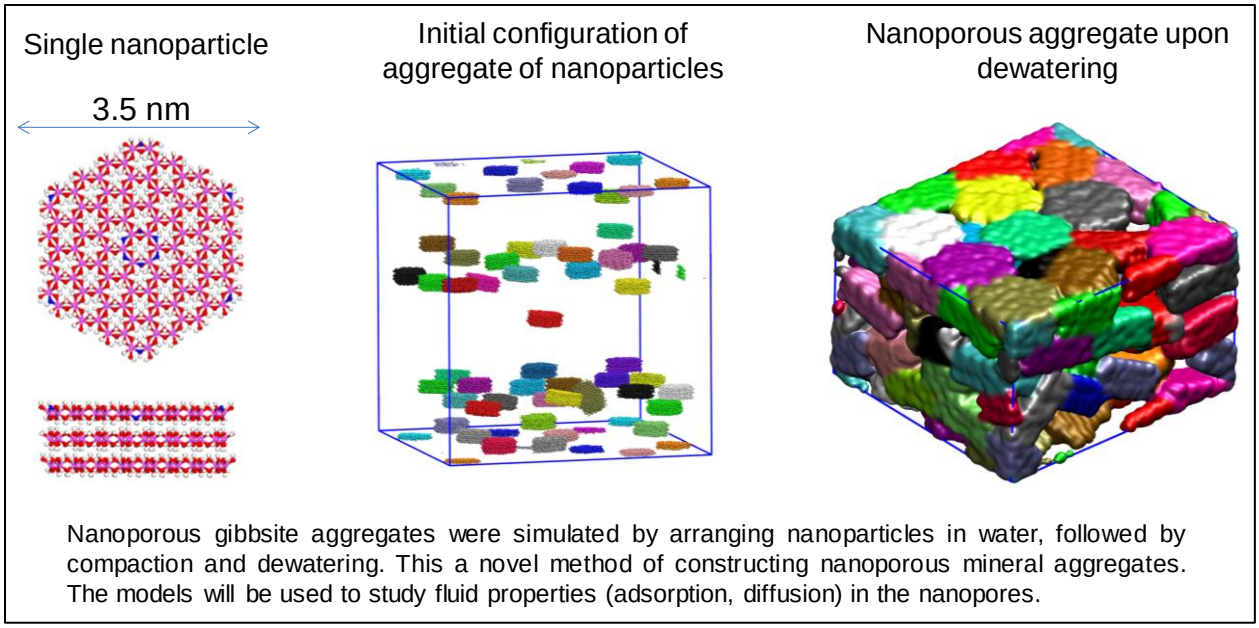

Nanoporous gibbsite aggregates were simulated by arranging nanoparticles in water, followed by compaction and dewatering. This a novel method of constructing nanoporous mineral aggregates. The models will be used to study fluid properties (adsorption, diffusion) in the nanopores.

Selected Recent References

Ilgen AG and Trainor TP (2016) Homogeneous oxidation of Sb(III) by aqueous O_2: the effect of ionic strength, Pb^{2+}, and EDTA. *Environ. Chem.* 13, 936-944 [**invited**]

Ilgen AG, Kukkadapu RK, Dunphy DR, Artyushkova K, Cerrato JM, Kruichak JN, Janish MT, Sun CJ, Argo JM, and Washington RE. (2017) Synthesis and characterization of redox-active ferric nontronite. *Chem. Geol.*, in press.

Leung K and Criscenti LJ. (2017) Selenite adsorption at water-goethite interfaces from first principles. *J. Phys. Condens. Mat.*, in press.

Pouvreau M, Greathouse JA, Cygan RT, and Kalinichev AG (2017) Structure of hydrated gibbsite and brucite edge surfaces: DFT results and further development of the ClayFF classical force field with metal O H angle bending terms. *J. Phys. Chem. C*, in press. DOI 10.1021/acs.jpcc.7b05362.

Ilgen AG, Kruichak JN, Artyushkova K, Newville MG, and Sun CJ. (2017) Redox transformations of As and Se at the surfaces of natural and synthetic ferric nontronites: role of structural and adsorbed Fe(II). *Environ. Sci Technol.*, submitted.

Ho TA, Greathouse JA, Wang Y, and Criscenti LJ (2017) Structural properties of clay-like nanoparticle aggregates under compaction and dewatering from molecular dynamics simulation. In preparation.

Sandia National Laboratories is a multimission laboratory managed and operated by National Technology and Engineering Solutions of Sandia LLC, a wholly owned subsidiary of Honeywell International Inc. for the U.S. Department of Energy's National Nuclear Security Administration under contract DE-NA0003525.

Real-time observations of cation exchange at the muscovite (001) – water interface

Sang Soo Lee,[1] Paul Fenter,[1] Kathryn L. Nagy,[2] and Neil C. Sturchio[3]

[1] Chemical Sciences and Engineering, Argonne National Laboratory, Argonne, IL 60439
[2] Department of Earth and Environmental Sciences, University of Illinois at Chicago, Chicago, IL 60607
[3] Department of Geological Sciences, University of Delaware, Newark, DE 19716

The mineral–water interface is a primary site for various geochemical reactions including ion adsorption/desorption and mineral growth/dissolution. Real-time observations can provide a fundamental basis for understanding reaction mechanisms at the interface. Temporal variations in the speciation and coverage of Rb^+ adsorbed at the muscovite (001) – water interface were monitored during its exchange with competing ion Na^+ using time-resolved resonant anomalous X-ray reflectivity. The desorption of Rb^+ occurred as a stepwise process in which thermodynamically stable inner-sphere Rb^+ transformed to less stable outer-sphere Rb^+ before desorption from the interface. In contrast, the adsorption of Rb^+ appeared to proceed directly to the dominant inner-sphere species within the experimental time resolution (~1 sec). Temperature-dependent measurements from 9 to 55°C were used to define the elementary rate constants of these processes, revealing that slow desorption is the rate limiting step for ion exchange at the interface. These results provide unique insights into the cation free energy profile at this charged mineral–water interface.

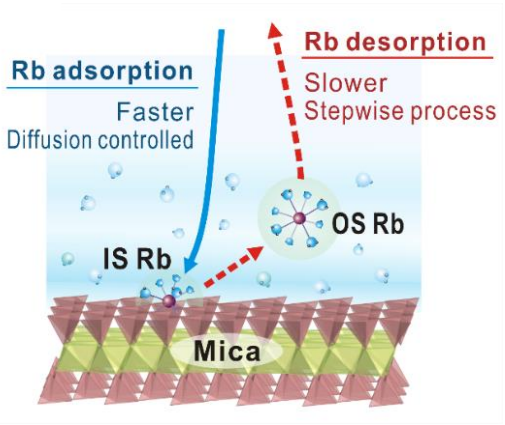

Figure: Schematic illustration of the path-dependent reaction that controls the reaction kinetics of ion exchange at the muscovite–water interface.

Comparison of H_2O and Sr^{2+} positions on barite (001) studied by atomic-scale simulation and X-ray scattering

James D. Kubicki (University of Texas at El Paso); Jacquelyn N. Bracco, Sang Soo Lee and Paul Fenter (Argonne National Laboratory); Andrew G. Stack (Oak Ridge National Laboratory)

Barite ($BaSO_4$) plays a role in geochemical process and is especially problematic in scaling of oil well production pipes. In addition, it serves as an excellent model material for similar minerals such as carbonates and sulfates because the surfaces are relatively stable. This talk will focus on recent X-ray scattering results using crystal truncation rod (CTR) and resonant anomalous X-ray reflectivity (RAXR) measurements that probe atomic positions at mineral-water interfaces. CTR is primarily used to probe the 3-dimensional structure of the interface including the locations of Ba and SO_4 groups and H_2O molecules near the crystal surface, and RAXR is used for determining positions of adsorbed Sr^{2+} ions. Both techniques are powerful analytical tools for deciphering mineral-water interface structures; however, the data can be challenging to interpret and benefit from independent computational results, both as an initial model and as a test of the accuracy of the conclusions.

We have used density functional theory (DFT) calculations on a periodic (001) barite surface to complement the X-ray scattering results. Model systems of 48 $BaSO_4$ + 195 H_2O and 48 $BaSO_4$ + 192 H_2O + Sr^{2+} + 2 Cl^- were first energy minimized then run in MD simulations using VASP, the gradient-corrected exchange correlation functional PBE and plane wave (PW) basis sets using projector-augmented wave (PAW) pseudopotentials with an energy cut-off of 500 eV and a Grimme D3 dispersion correction. MD simulations were run at 298 and 381 K with a time step of 0.5 fs in an NVT ensemble. The large simulation cell size (17.768x16.374x33.5692 $Å^3$) allowed for the use of 1 Γ-centered k-point.

The DFT results reproduce the first two O atom vertical positions for H_2O above the (001) barite surface (1.86 CTR vs 1.80 Å DFT and 2.42 CTR vs 2.60 Å DFT), but the third position is significantly farther from the surface in DFT compared to CTR (3.52 vs 4.0 Å). In addition, the first 3 peak intensities are stronger in the CTR compared to DFT, and the DFT model produces peaks near 6, 9 and 11 Å that are not observed with CTR. There are 3 main potential reasons for these discrepancies:

1. inaccuracy of the DFT methodology,
2. limited run time in which the DFT-MD does not reach equilibrium, and
3. limited system size of the DFT model constrains mineral-water interface configurations.

Each of these factors is likely to play a role to some degree. Hence, it is imperative that we refine classical force fields to better reproduce the observed data while allowing for larger spatial and longer temporal scales to be included in the MD simulations. The current classical MD simulations are not as accurate compared to the CTR as the DFT-MD simulations, so improvements in the force field parameterization are necessary.

RAXR results have been interpreted as Sr^{2+} adsorption occurring at 1.04 to 1.22 Å above the plane of the highest Ba^{2+} ions on the surface. DFT simulations predict that the inner-sphere mode of adsorption would have the Sr^{2+} adsorption 2.2 ± 0.2 Å above this surface with an outer-sphere Sr^{2+} at 4.8 ± 0.2 Å. This outer-sphere mode is not observed in the RAXR results. This discrepancy in the inner-sphere Sr^{2+} height is being addressed in two ways. First, the RAXR results are being re-interpreted using the DFT models as a basis. Second, the DFT models have been revised to bond the Sr^{2+} to 2 O atoms of different SO_4^{2-} groups on the surface at a height of ~1 Å above the Ba^{2+} plane. In addition, Cl^- has been moved to form an ion pair with the Sr^{2+}. The Sr^{2+}-Cl^- bond is weaker than the Sr^{2+}-OH_2 bond, so this may allow the Sr^{2+} to form a stronger and shorter bond to the surface O atoms and help resolve the experimental/computational discrepancy.

Unraveling Interfacial Atom and Electron Exchange Mechanisms in Fe(II)-Catalyzed Fe(III)-Oxide Recrystallization

Kevin M. Rosso

Pacific Northwest National Laboratory, Washington, U.S.A.
kevin.rosso@pnnl.gov

Understanding Fe(II)-catalyzed transformations of Fe(III)-(oxyhydr)oxide minerals such as ferrihydrite, goethite, and hematite is critical for correctly interpreting stable isotopic distributions and for predicting the fate and mobility of trace, heavy and radioactive metal ions in the environment. The iron system is also a key archetype for understanding the geochemical cycling of redox-active elements in natural waters and in the subsurface in general. Across redox gradients, changes in the electrochemical potential impact iron speciation and distribution, juxtaposing soluble Fe(II) against Fe(III)-oxide solids. This contact is dynamic, catalysing recrystallization of even the most stable Fe(III) mineral forms and enabling iron atom exchange across the interface. The underlying electron transfer (ET) step between sorbed Fe(II) and oxide Fe(III) is one of the most fundamental yet elusive geochemical processes to directly probe.

Macroscopic isotopically labelled ^{57}Fe tracer studies suggest that recrystallization is facile and involves a moving front through oxide mineral interiors. Solid-state electron mobility through these minerals appears to play a role, linking spatially distinct oxidative growth and reductive dissolution reactions across nanophase crystallites. Monte Carlo simulations of diverse macroscopic tracer mixing data for ^{57}Fe(II)/^{NA}goethite as a function of particle size and pH show that the entire data set can be explained in terms of a systematic pH dependence of the density of sorbed Fe(II) sites, where interfacial ET presumably occurs. The underlying atom exchange rate constant of 10^{-5} Fe nm^{-2} s^{-1} is consistent with the proposed conduction mechanism of recrystallization, and implies that the reductive dissolution step is rate limiting.

In a first attempt to directly probe the atom exchange front, we explored use of APT and nanoSIMS to map the spatial distribution of the ^{57}Fe tracer on individual crystallites in the ^{57}Fe(II)/^{NA}hematite system. Analyses of the mass spectrum with respect to natural abundance recovery at depth show clear ^{57}Fe enrichment at the surface within the uppermost nm of the (001) surface. 3D reconstructions show that the atom exchange front is spatially heterogeneous across the surface, consistent with nanoislands of oxidative growth. Single crystal nanoSIMS maps show strong preferential tracer enrichment on the (001) surface relative to higher energy (012) edge facets and defect-rich granular intergrowths. The collective findings indicate that ET-enabled atom exchange involves coupled oxidative growth and reductive release each occurring at specific crystallite facets, in a manner consistent with the conduction-based mechanistic basis for recrystallization.

Kinetics of redox reactions of actinides on semiconducting minerals, as well as studtite and U_{60} clusters

Udo Becker (PI), Ke Yuan, YoungJae Kim, Ben Gebarski, Will Bender
University of Michigan, Earth and Environmental Sciences, Ann Arbor, MI 48109
Email: ubecker@umich.edu

1. *Resolve kinetics of adsorption/reduction into sub-processes such as bulk diffusion in bulk solution, surface diffusion, stripping of hydration sphere, adsorption, overcoming activated states due to incompatible orbital symmetries or spin transitions.*

Bulk diffusion rate in solution was approximated by collision theory for reaction of actinyl ions with reactants such as hydroxyl radicals, OH-, HS-, and ferrous iron. Outer-to-inner sphere complex transitions kinetics was determined using distance-dependent energy profiles.

2. *Use a combination of quantum-mechanical calculations, electrochemical powder micro-electrode measurements, batch experiments with subsequent TEM, XPS, and ICP-MS analysis, and electrochemical AFM measurements to resolve overall reaction path and mechanism and evaluate which of the sub-processes controls kinetics as function of environmental parameters (pH, pe, T, solution chemistry, and light).*

Electrochemical experiments were instrumental in determining redox mechanisms and kinetics as a function of pH and solution concentration. An extended theory was developed along the experiments, on how solution speciation chemistry controls pH shift of redox transitions and more complex mechanisms were included for the pe-pH dependence of mineral-catalyzed reactions.

Electron transfer kinetics across actinide-mineral interfaces: In order to understand the atomistic mechanism and kinetics of actinyl redox processes, quantum-mechanical electron transfer calculations involving Marcus theory have been performed. Electron-transfer (ET) calculations on the first rate-limiting ET-step (the reduction of U(VI)aq to U(V)aq by Fe(II)aq) complement the experimental results. The homogeneous reduction of U(VI)aq to U(V)aq by Fe(II)aq is thermodynamically and kinetically favorable if an inner–sphere complex can be achieved. However, significant thermodynamic and kinetic barriers exist to proceed from an outer–sphere ET reaction to an inner–sphere ET reaction, a process that needs to overcome dehydration of the first solvation shell and hydrolysis of Fe(II)aq.

3. *Move on to metal organic frameworks (MOFs) and actinyl nanoclusters and their redox, electronic, and catalytic properties.*

MOFs have been treated quantum-mechanically in combination with a thermodynamic approach to understand the relative stability of certain MOFs with respect to different actinides and subsequently, to understand the electronic structure as a function of the linker and the actinide to get an impression of the capability as redox catalysts. U60 nanoclusters have been studied extensive, also in comparison to their mineral analogue studtite and the kinetics and redox potential have been determined as a function of pH and solution chemistry. Attempts were made to determine if the U in the nanoclusters switch oxidation state with the cluster being

4. *Use the information gained to help developing a strategy for optimizing reaction conditions for given applications, such as actinyl immobilization in permeable reactive barriers or geologic barriers near nuclear waste repositories, and to understand the geochemical behavior of actinyl phases in the environment.*

We are on our way in developing a more comprehensive way of deconvoluting reaction mechanism that helps understand what subprocesses control kinetics under what conditions which may be crucial to develop more reliable predictive models.

Iron Redox and Photo-redox Reaction Mechanism from Time-Resolved Spectroscopy

Benjamin Gilbert[1,] David. M. Mangiante[1], Richard D. Schaller[2], Piotr Zarzycki[1,3], Jillian F. Banfield[1,4], Jennifer Soltis[5], Adam Schwartzberg[6], R. Lee Penn[5] and Kevin M. Rosso[7]*

[1]Energy Geoscience Division, Lawrence Berkeley National Laboratory, 1 Cyclotron Road, Berkeley, CA 94720
[2]Center for Nanoscale Materials, Argonne National Laboratory, 9700 South Cass Avenue, Building 440, Argonne, IL 60439, USA
[3]Institute of Physical Chemistry, Polish Academy of Sciences, Warsaw, Poland
[4]Department of Earth and Planetary Science, University of California – Berkeley, Berkeley, CA 94720
[5]Department of Chemistry, University of Minnesota, Minneapolis, Minnesota 55455, United States
[6]Molecular Foundry, Lawrence Berkeley National Lab, Berkeley, California 94720 United States
[7]Physical Sciences Division, Pacific Northwest National Lab, Richland, WA 99354
*Corresponding author: bgilbert@lbl.gov

Thermal and light-driven redox reactions of aqueous iron species and iron minerals play numerous important roles in terrestrial and subsurface biogeochemical processes, including the carbon cycle. Mechanistic understanding of iron cycling is important to anticipate environmental responses under changing conditions. Time-resolved spectroscopic approaches can provide insight into geochemical reaction mechanism by providing snapshots of transient intermediates. We review recent results in determining the mechanisms of iron redox reaction. Iron(III) oxalate, $Fe^{3+}(C_2O_4)_3^{3-}$, is a photoactive metal organic complex found in natural systems that undergoes optical-light photolysis to form CO_2. We employed pump/probe mid-infrared transient absorption spectroscopy to study the photolysis reaction of the iron(III) oxalate ion in D_2O and H_2O up to 3 ns following photoexcitation. We tracked the formation and fate of reaction intermediates, including the radical anion $CO_2^{\bullet-}$, and clarify the reaction pathway.

Ferrihydrite, a nanophase and poorly crystalline Fe(III)-oxyhydroxide, plays an important role in controlling contaminant and nutrient availability because reductive dissolution readily releases surface-bound species. We have shown that electrons at Fe(II) sites in ferrihydrite are mobile through a nanosecond-timescale hopping process, and hypothesized that internal conduction is a

rate limiting step for some reactions. We acquired optical transient absorption spectra as a function of particle size and under a variety of solution conditions, and find evidence for electron trapping that dominates conduction and reaction on millisecond timescales.

[1] D. M. Mangiante, R. D. Schaller, P. Zarzycki, J. F. Banfield and B. Gilbert. Mechanism of ferric oxalate photolysis. *ACS Earth and Space Chemistry* (in press). 10.1021/acsearthspacechem.7b00026

[2] J. A. Soltis, A. M. Schwartzberg, P. Zarzycki, R. L. Penn, K. M. Rosso and B. Gilbert Electron Mobility and Trapping in Ferrihydrite Nanoparticles. *ACS Earth and Space Chemistry* (in press). 10.1021/acsearthspacechem.7b00030

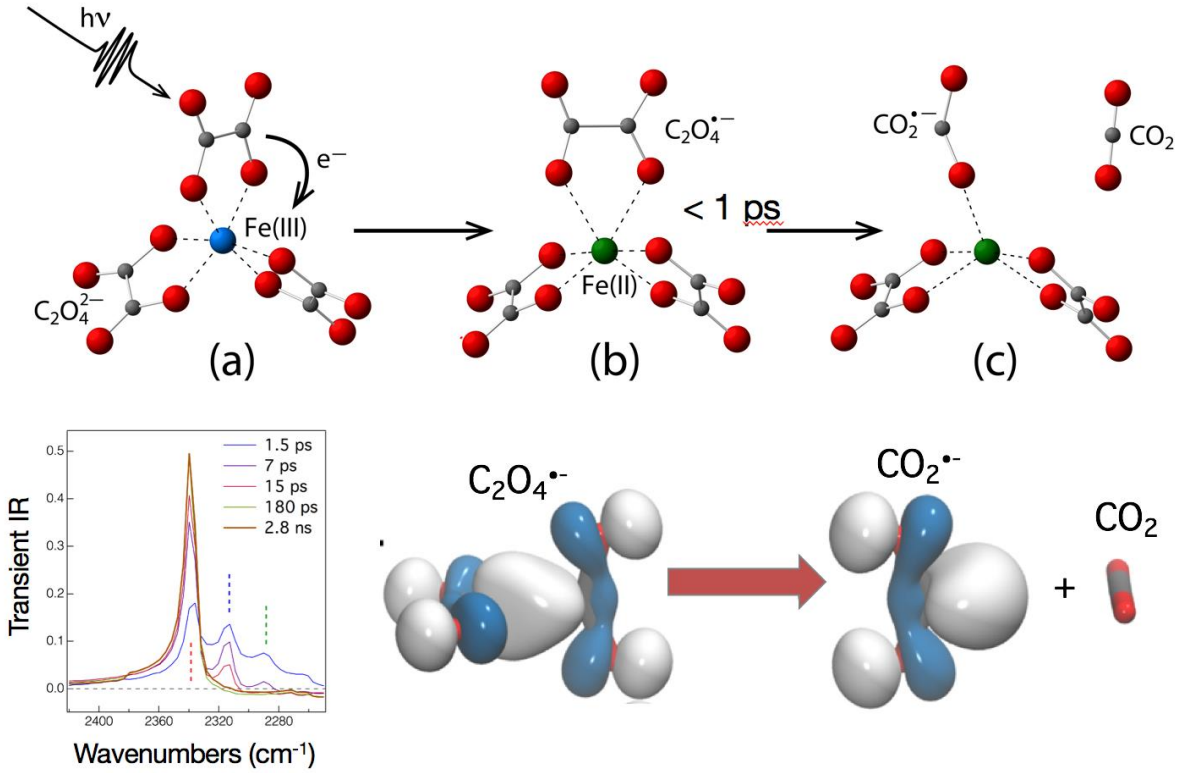

Diffusion and solubility of volatiles in cryptocrystalline materials and simple oxides: CO_2 and N_2 in chert and C isotopes in polycrystalline MgO

Elizabeth Pettitt*, Morgan F. Schaller†, E. Bruce Watson#

The broad thrust of the BES program at RPI is to develop new experimental and analytical strategies to quantify the capacity of crustal materials to store and transport carbon and nitrogen. The overarching goals are: 1) to assess the capability of underexploited near-surface materials such as cherts to retain information on the composition of ancient atmospheres; and 2) to improve our understanding of the role of crystalline silicates and oxides in the geochemical cycling of C and N. Here we focus on C and N diffusion in chert and C in polycrystalline MgO.

Diffusion measurements on polished chert specimens were conducted using two different techniques—one involving in-diffusion from an external C-O-H-N gaseous atmosphere, the other utilizing ion implantation followed by thermal annealing. In both cases, C and N diffusion profiles were characterized directly by nuclear reaction analysis (NRA) and the profiles fit to appropriate diffusion models to extract diffusivities. The two experimental techniques yield consistent results, and reveal that diffusion behavior in chert at 250-450°C is similar for C and N species (coincidentally, both are also similar to N diffusion in obsidian, which we have also characterized). The data exhibit more scatter than is typical of the well-defined Arrhenius lines for minerals, which is believed to be a consequence of the inherent variability of chert at the micro- and nano-scale. Extrapolated to Earth-surface conditions, diffusion in chert is sufficiently slow that atmospheric CO_2 and N_2 trapped during chert formation should be effectively retained over vast geologic time. To complement the diffusion studies, we have developed the capability to measure CO_2 and N_2 in natural cherts at the pico-mole level using a newly-developed online crushing technique combined with quadrupole and isotope ratio mass spectrometry. Natural cherts contain variable but easily-measured levels of N_2 and CO_2.

Our studies of C transport in polycrystalline MgO have focused on grain-boundary diffusion and accompanying isotopic fractionation. Absence of porosity is essential to the interpretation of the measurements, so the experiments are conducted at ~1 GPa in a piston-cylinder apparatus. This poses a major complication because the graphite tubular heating element (furnace) of a piston-cylinder pressure assembly is made of the element whose diffusion properties we seek to characterize. This complication inspired a new diffusion cell design in which the furnace tube itself serves as the source of diffusant C atoms, which migrate radially from the inner surface of the furnace tube through a cylindrical sample of polycrystalline MgO filling the tube. Carbon atoms are "captured" by a Ni wire placed along the axis of the MgO cylinder (C is slightly soluble in Ni). Following a diffusion experiment, the concentration and isotopic character of C in the Ni wire and MgO are measured by EA IRMS, and diffusive fluxes calculated from the number of C atoms transferred. Results to date at 1200°C reveal that $\delta^{13}C$ of the C in the MgO and Ni wire is ~2‰ lower than the graphite furnace, which implies diffusive fractionation of C isotopes in MgO grain boundaries through faster migration of ^{12}C relative to ^{13}C. On the basis of these preliminary measurements, we suggest that grain boundary diffusion of C species in natural systems may result in substantial isotopic fractionation.

---

* PhD student
† Co-I
# PI

Insights into geochemical transformations probed by examining solution and solid phase structures using neutron diffraction and atomic-scale simulation

Andrew G. Stack, Hsiu-Wen Wang, Luke L. Daemen, Jörg Neuefeind, Katharine L. Page, Nikhil Rampal, J. Michael Simonson, Lukas Vlcek

The focus of this talk will be on the structures of hydrated amorphous calcium carbonate and solutes in aqueous solutions studied by combined neutron diffraction and atomic-scale simulation. This topic is important because the mechanisms by which nucleation and crystallization reactions occur are not clear and are thus a major focus of geochemical and materials research. Classical models of these transformations rely on macroscopic properties, such as interfacial energies, to make predictions. However, there is wide variability in interfacial energy measurements and large energy barriers to nucleation are predicted. Based in part on the latter issue, some recent work has suggested that non-classical nucleation pathways are more likely. These include formation of pre-nucleation clusters and precipitation of amorphous phases as a pre-cursor to crystal formation. Here, I will focus on using neutron and X-ray pair distribution function methods (nPDF, XPDF) to examine structure of an amorphous material and the hydration structure of aqueous ions with the specific goal of looking for ion pair and cluster formation and making inferences about crystallization pathways.

Firstly, the structure of amorphous calcium carbonate (ACC) will be examined. Since hydrogen detrimentally interferes with nPDF analysis, a major accomplishment was simply synthesizing a deuterated sample in sufficient quantities for nPDF. The results reveal the positions of Ca-O, Ca-D and O-O to which XPDF is less sensitive. In heating this sample, we observe a transition from ACC to crystalline portlandite and lime in addition to calcite. Comparison to TGA-MS suggests that a component of this ACC is calcium deuteroxide. If this finding is universal, calcium hydroxide may play a role in stabilizing the amorphous structure rather than the crystalline phases.

I will also discuss the structure of hydrated aqueous nitrate ion, and aqueous calcium chloride, sodium chloride, and zinc chloride. The structure of oxyanions in general is not well constrained, so working to understand the structure of nitrate is a useful test case. A poorly structured hydration shell is observed around nitrate, which is rationalized by its relatively small hydration free energy. For the chloride systems, we only observe ion pair formation in zinc chloride, where it is expected, but not ion pair formation is detected in sodium chloride or calcium chloride. Combined, the results suggest that cluster formation is not detected despite being concentrated solutions, and distinct ion pairs are only observed in systems where they are already known to occur (zinc chloride, but not calcium or sodium chloride).

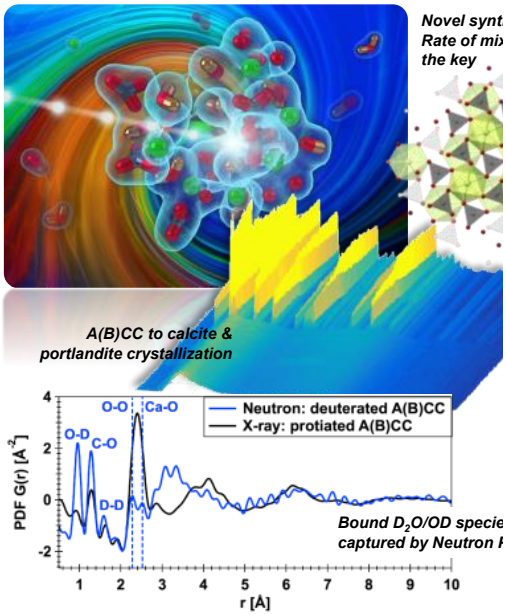

Neutron diffraction has been used to study the structure of amorphous calcium carbonate and its transformation to calcite, portlandite and lime.

Wang, H.-W.; Daemen, L. L.; Cheshire, M. C.; Kidder, M. K.; Stack, A. G.; Allard, L. F.; Neuefeind, J.; Olds, D.; Liu, J.; Page, K. (2017) *Chem. Comm.* 53, 2942-2945. DOI: 10.1039/C6CC08848A

Reactive Molecular Dynamics as a Unique Tool for Understanding Reactivity of Mineral surfaces: Fe(II)-catalyzed Recrystallization of Goethite

Piotr Zarzycki[1*] and Kevin M. Rosso[2]
[1]Energy Geoscience Division, Lawrence Berkeley National Laboratory, Berkeley, CA
[2]Pacific Northwest National Laboratory, Richland, WA
*e-mail: ppzarzycki@lbl.gov

Trace element and radionuclide transport and speciation are controlled by the acid-base and charge-transfer reactions occurring at the mineral/aqueous solution interface – in particular at the most reactive iron oxide mineral surfaces. These charged interfaces are able to degrade environmental pollutants thanks to a facile Fe^{2+}/Fe^{3+} redox transformation. However, knowledge gaps regarding the interplay between pH, sorption processes and redox reactions limit our ability to predict and use redox-based remediation strategies.

A long-standing challenge is to incorporate electron and proton transfer reactions in simulation methods without deteriorating the efficiency offered by classical molecular dynamics (MD). Here, we illustrate how reactive simulation methods can provide a molecular level understanding of Fe(II) catalyzed goethite recrystallization – an important case study system [1-3].

We combine the constant-pH molecular dynamics approach [4] that allows us to efficiently explore simultaneously protonation space via Monte Carlo sampling and configuration space via classical molecular dynamics. We also added the Kinetic Monte Carlo steps to model the oxide growth/dissolution. Using this reactive-hybrid MD approach, we find that iron exchange between aqueous Fe(II) and solid Fe(III) is controlled by the coupling between the surface charge dynamics, particle morphology, sorption, and electron-transfer energetics. All controlling variables are strongly pH- and crystal-face dependent.

The reactive MD approach successfully describes Fe(II)-driven iron oxide recrystallization and could be extended to full simulations of radionuclide immobilization. It could further be used to tackle a broad range of biogeochemical systems, including the protonation, conformation and redox properties of proteins, the adsorption of natural organic molecules to mineral surfaces.

[1]. Handler, R. M., et al. (2014). Fe(II)-Catalyzed Recrystallization of Goethite Revisited. *Environ. Sci. Technol., 48*(19), 11302–11311.
[2]. Joshi, P., Gorski, C. A. (2016). Anisotropic Morphological Changes in Goethite during Fe^{2+}-Catalyzed Recrystallization. *Environ. Sci. Technol.*, *50*(14), 7315–7324.
[3]. Zarzycki, P., Rosso, K. M. (2017). Stochastic Simulation of Isotopic Exchange Mechanisms for Fe(II)-Catalyzed Recrystallization of Goethite. *Environ. Sci. Technol.*, *51*(13), 7552–7559.
[4]. Zarzycki, P., Smith, D. M., Rosso, K. M. (2015). Proton Dynamics on Goethite Nanoparticles and Coupling to Electron Transport. *J. Chem. Theory Comput.*, *11*(4), 1715–1724.

Imaging Reactions at Morphologically Complex Mineral – Water Interfaces

Ke Yuan[1], Vincent De Andrade[2], Neil C. Sturchio[1], Sang Soo Lee[1], Paul Fenter[1]

[1] Chemical Sciences and Engineering, Argonne National Laboratory, Argonne, IL 60439
[2] Advanced Photon Source, Argonne National Laboratory, Argonne, IL 60439
[3] Department of Geological Sciences, University of Delaware, Newark, DE 19716

A robust understanding of the processes at mineral-water interfaces, such as dissolution/crystallization, is central to a broad range of geochemical reactions. Here, we report on efforts to understand reactions at non-ideal mineral-water interfaces. Our initial focus is on reactions of individual crystallites (sub-micron to few-micron in size) to understand the role of spatial morphology, strain fields and structural relationships between the secondary phase and the host mineral at conditions at conditions where the host mineral is undersaturated with respect to the reaction solution. We used a set of emerging X-ray imaging techniques, such as Transmission X-ray microscopy (TXM) and Bragg coherent diffractive imaging (BCDI) which are compared to parallel studies by X-ray reflectivity. The complex inter-relationships between the host mineral and secondary phases were obtained through investigations of the pseudomorphic mineral growth of cerussite and lipidocrocite on calcite that were imaged at 60 nm resolution by TXM. Reactions of magnetite in acidic solution (e.g., leading to the leaching of Fe(II)) were imaged by BCDI to reveal the combined morphology and 3D atom displacement field (i.e., strain) of nano magnetite crystals as a function of reaction time.

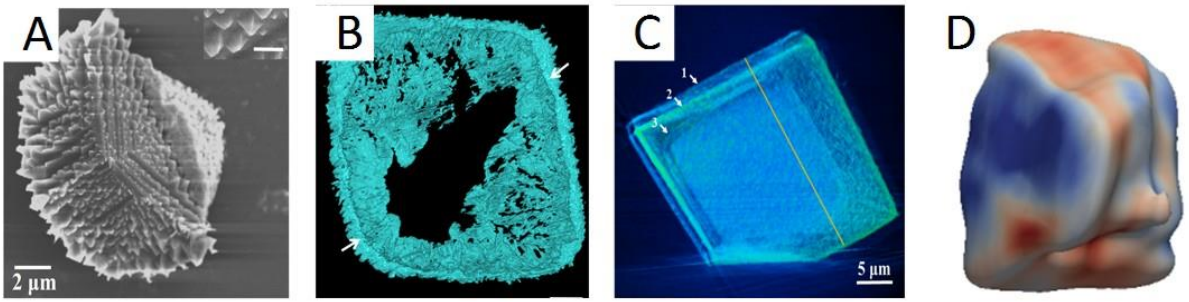

Figure: Morphologies of individual mineral grains including calcite reacted with Pb^{2+} solutions for short and long reaction times (image by SEM and TXM, respectively), calcite reacted with Fe^{2+} solutions (imaged by TXM) and strain fields (expressed in color) and grain shape in a magnetite grain that has been partially dissolved in acidic aqueous solutions.

Genesis, Storage, Producibility, and Natural Leakage of Shale Gas

A. Schimmelmann (aschimme@indiana.edu), M. Mastalerz (mmastale@indiana.edu), and J. Schieber (jschiebe@indiana.edu), Indiana University, award Number DE-SC0006978.

Shales are important source and reservoir rocks for shale gas. Three research goals of this project encompass: **(1)** testing of shales' ability to generate natural gas at relatively low temperatures *via* catalysis; **(2)** quantification of the character and development of porosity in shales; and **(3)** evaluation of natural outgassing of methane from shales into the atmosphere.

(1) The hypothesis of catalytic gas generation from shales in the absence of methanogenic microbes has been tested at 60 and 100 °C by long-term (6 months to 5 years) heating of pre-evacuated and sterilized shales. It was demonstrated that low-temperature abiogenic methanogenesis does occur at laboratory conditions, and may explain the occurrence of non-biogenic natural gas plays where insufficient thermal maturity contradicts the conventional thermal cracking paradigm (Wei, 2016; Wei et al., in review). Experimental methane yields at 60 and 100 °C are 5 to 11 orders of magnitude higher than the theoretically predicted yields from kinetic models of thermogenic methanogenesis (Fig. 1). Regardless of remaining quantitative uncertainty, our data let us conclude that catalytic methanogenesis in shales is active and should be considered when prospecting for shale gas in thermally immature basins.

(2) Porosimetry data from low pressure gas adsorption, mercury porosimetry, small-angle neutron scattering, and SEM imaging were used to assess macro-, meso- and microporosity in shales in relation to maturation and compaction. The influence of temperature and pressure on the evolution of meso and microporosity in shales was tested in experiments of 6 to 12-month duration and at temperatures of 60, 100, and 200 °C, and pressures up to 300 MPa. Increased hydrostatic or lithostatic pressure did not notably affect pores <100 nm, in contrast to more susceptible larger pores (Drobniak et al., in press). An optimal size fraction was empirically determined to obtain realistic and comparable results *via* gas adsorption porosimetry (Mastalerz at al., 2017). Ion-milling techniques of shale SEM samples without cautionary cooling can thermally stress shale surfaces, elevate maturity and artificially change porosity.

(3) Natural outgassing of shale gas into the atmosphere in the absence of drilling and hydraulic fracturing was evaluated during international field work. Our original description of natural gas seeps in New York State (Etiope et al., 2013) gained relevance in June 2017 with our discovery of an even larger macroseepage system at a distance of a few kilometers. However, the abundance of natural hydrocarbon seepages in New York State that is fed by deeper shales through tectonically-induced geologic faults as conduits seems to be geologically atypical and not matched by any other region in the world. Our international field work in 49 caves and published data from ~10 mostly European caves established that methane in subterranean air is typically depleted relative to the atmosphere. Only a cave in a volcanic region in Mexico featured a small influx of thermogenic hydrocarbon gas (Webster et al., in press). Cave systems are often aligned with geologic faults that would funnel seeping natural gas from below into cave air before surface winds can dilute the signal. Our data indicate that seepage of natural gas does not result in significant outgassing of methane into cave air or the atmosphere (Webster et al., 2016; Nguyễn-Thuỳ et al., in press). Only exceptionally strong fluxes of rising natural gas (e.g., in New York State) can overwhelm the omnipresent methanotrophic uptake of methane by microbes in the vadose zone and soils (Lennon et al., 2017).

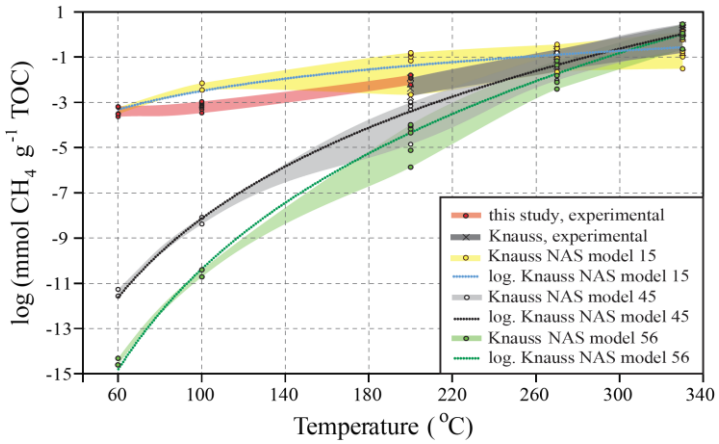

Figure 1: Decadal logarithms of experimentally observed and kinetic model CH_4 yields (mmol CH_4 g^{-1} total organic carbon, TOC) *versus* temperature of experimental/model predictions for New Albany Shale. The figure compares our experimental results with data from two kinetic models (Knauss et al., 1997). Ranges in model/experimental CH_4 yields for a given temperature are indicated by vertical widths of color bands. This uncertainty is partially due to differences in duration of experiments and model runs ranging from days to months. The experimental temperature of 60 °C approximates the current temperature for New Albany Shale. The kinetics of our experimental CH_4 generation at 60 °C are orders of magnitude faster than those predicted by traditional kinetic models, and thus suggest catalysis. Extrapolation of experimental CH_4 generation over geologic time would rapidly convert TOC in shale to methane within a few hundred thousand years.

References with embedded electronic DOI etc. links:

Drobniak A, Mastalerz M, Wei L, Schimmelmann A, Schieber J (in press) Maturity and porosity of kerogen Type II and III during gas generation at varying pressure and temperature. *34th Annual Meeting of The Society for Organic Petrology* (TSOP), September 21-27, 2017, Calgary, Canada (abstract).

Etiope G, Drobniak A, Schimmelmann A (2013) Natural seepage of shale gas and the origin of "eternal flames" in the Northern Appalachian Basin, USA. *Marine and Petroleum Geology* **43**, 178-186.

Knauss KG, Copenhaver SA, Braun RL, Burnham AK (1997) Hydrous pyrolysis of New Albany and Phosphoria Shales: Production kinetics of carboxylic acids and light hydrocarbons and interactions between the inorganic and organic chemical systems. *Organic Geochemistry* **27** (7-8), 477-496.

Lennon JT, Nguyễn-Thùy D, Phạm TM, Drobniak A, Tạ PH, Phạm NĐ, Streil T, Webster KD, Schimmelmann A (2017) Microbial contributions to subterranean methane sinks. *Geobiology* **15** (2), 254-258.

Mastalerz M, Hampton L, Drobniak A, Loope H (2017) Significance of particle size in low-pressure N_2 and CO_2 adsorption of coal and shale. *International Journal of Coal Geology* **178**, 122-131.

Nguyễn-Thuỳ D, Schimmelmann A, Nguyễn-Văn H, Drobniak A, Lennon JT, Tạ PH, Nguyễn NTÁ (in press) Subterranean microbial oxidation of atmospheric methane in cavernous tropical karst. *Chemical Geology*.

Webster KD, Mirza A, Deli JM, Sauer PE, Schimmelmann A (2016) Consumption of atmospheric methane in a limestone cave in Indiana, USA. *Chemical Geology* **443**, 1-9.

Webster KD, Rosales Lagarde L, Sauer PE, Schimmelmann A, Lennon JT, Boston PJ (in press) Isotopic evidence for the migration of thermogenic methane into Cueva de Villa Luz, Tabasco, Mexico. *Journal of Cave and Karst Studies*.

Wei L (2016) *Gas Genesis and Storage in Source Rocks: Geochemistry, Organic Petrology and Porosimetry*. Ph.D. Dissertation, Indiana University.

Wei L, Schimmelmann A, Mastalerz M, Lahann RW, Sauer PE, Drobniak A, Strąpoć D, Mango FD (in review) Catalytic generation of methane at 60 to 100 °C and 0.1 to 300 MPa from source rocks containing kerogen Types I, II, and III. *Geochimica et Cosmochimica Acta*.

Investigating the Roughness and Advance Rate of the Weathering Interface:

Shale, Schist, Diabase, Granite, Volcaniclastics, and Serpentinite

S.L. Brantley, X. Gu, V. Marcon, H. Kim, M. Lebedeva

Pennsylvania State University, Earth and Environmental Systems Institute, Univ. Pk PA 16802

As part of our effort to understand how water enters rocks during weathering, we are using neutron scattering to understand porosity in rocks of different lithology and in different environmental conditions. We have investigated shales, schist, diabase, granite, volcaniclastics, and serpentinite to learn how lithology affects porosity growth in rocks as they weather under conditions of low erosion rate. We also compare the effects of high erosion rate on shale. The objectives of the project are to learn how chemical reactions, fracturing, and porosity growth inter-relate as weathering creates regolith.

This presentation will review some of our findings over the last year. The six main findings of our DOE-funded work through 2017 have been published in the peer-reviewed literature (Brantley et al., 2017; Gu and Mildner, 2016; Gu et al., 2016; Kim et al., 2017; Lebedeva and Brantley, 2017, in press; Liu et al., 2016; Reis and Brantley, 2017; Zachara et al., 2016) and are summarized here. 1) We have observed that the weathering advance rate depends on the roughness of the reaction front: specifically, the thickness and depth of the bedrock/regolith interface is larger where fracture spacing is smaller (other variables held constant). 2) Porosity in an unweathered crystalline rock is usually a mass + surface fractal that scatters neutrons isotropically. In contrast, porosity in an unweathered shale is usually a surface fractal that scatters neutrons anisotropically. 3) When other variables are maintained constant, regolith generally becomes thicker on rocks such as granites which often experience weathering-induced fracturing as compared to more massive mafic rocks that tend to not fracture during weathering. 4) Soil gases generate positive and negative feedbacks during weathering of granite and diabase respectively. 5) Deep weathering occurs in shale because oxidation of pyrite or organic matter initiates at depth and is often accompanied by calcite dissolution, and growth of this deep porosity accelerates access of meteoric waters into the rock. 6) In the shallow subsurface of catchments, water flows both vertically and laterally: water flows vertically in porous material that is water-unsaturated (resulting in wide reaction fronts), and water flows laterally wherever water perches intermittently on relatively impermeable layers (resulting in sharp reaction fronts).

Brantley, S.L., Lebedeva, M.I., Balashov, V.N., Singha, K., Sullivan, P.L., Stinchcomb, G., 2017. Toward a conceptual model relating chemical reaction fronts to water flow paths in hills. Geomorphology 277, 100-117, doi.org/110.1016/j.geomorph.2016.1009.1027.

Gu, X., Mildner, D.F.R., 2016. Ultra-small-angle neutron scattering with azimuthal asymmetry. Journal of Applied Crystallography 49, 934-943.

Gu, X., Mildner, D.F.R., Cole, D.R., Rother, G., Slingerland, R., Brantley, S.L., 2016. Quantification of organic porosity and water accessibility in Marcellus Shale using neutron scattering. Energy Fuels 30, 4438-4449.

Kim, H., Stinchcomb, G., Brantley, S.L., 2017. Feedbacks among O_2 and CO_2 in deep soil gas, oxidation of ferrous minerals, and fractures: A hypothesis for steady-state regolith thickness. Earth and Planetary Science Letters 460, 29-40.

Lebedeva, M., Brantley, S.L., 2017, in press. Weathering and erosion of fractured bedrock systems. Earth Surface Processes and Landforms.

Liu, W.J., Liu, C.Q., Brantley, S.L., Xu, Z.F., Zhao, T., Liu, T.Z., Yu, C., Xue, D.S., Zhao, Z.Q., Cui, L.F., Zhang, Z.J., Fan, B.L., Gu, X., 2016. Deep weathering along a granite ridgeline in a subtropical climate. Chemical Geology 427, 17-34.

Reis, F., Brantley, S.L., 2017. Models of transport and reaction describing weathering of fractured rock with mobile and immobile water. Journal of Geophysical Research-Earth Surface 122, 735-757.

Zachara, J., Brantley, S., Chorover, J., Ewing, R., Kerisit, S., Liu, C., Perfect, E., Rother, G., Stack, A., 2016. Internal domains of natural porous media revealed: Critical locations for transport, storage, and chemical reaction. Environmental Science & Technology, doi: 10.1021/acs.est.1025b05015.

Computational Studies of Geochemical Nanoparticles: A Bottom-Up Approach

David A. Dixon[1] and Mingyang Chen[2]
Department of Chemistry, The University of Alabama, Tuscaloosa, AL
Beijing Computational Science Research Center, Beijing, China

The primary effort of the work is the development of computational approaches for the prediction of the structure, stability, and reactivity of geochemical interfaces using electronic structure methods at the density functional theory (DFT) and correlated molecular orbital theory levels. We have developed a Tree-Growth-Hybrid Genetic Algorithm (TG-HGA) for structure building and finding global minima. The TG-HGA is used with different interaction potentials at each level with final energetics at the DFT level with appropriate exchange-correlation functionals benchmarked at the coupled cluster CCSD(T) level. We have used this bottom-up evolutionary approach to predict the structures of nanoclusters of MgO, $MgCO_3$, CaO, $CaCO_3$, and $Mg(OH)_2$. $(MgO)_n$ and $(CaO)_n$ form 3-D structures for $n > 3$ and cubic structures and their variations dominate for $n > 20$ consistent with formation of structures that are like the bulk. The TG-HGA was extended to deal with more complex monomers including carbonates and hydroxides. The most stable isomers for $(MgCO_3)_n$ and $(CaCO_3)_n$ ($n > 5$) are 3-D and are amorphous with structures derived from cuts of the crystal much higher in energy than the global minima. The formation of $Mg_xO_y(OH)_z$ nanoparticles leading to $Mg(OH)_2$ (brucite) nanoparticles were modeled in two steps: (1) formation of small $Mg_nO_{m+n}H_{2m}$ clusters via the hydrolysis of $(MgO)_n$ and (2) formation of multilayered $(MgO_2H_2)_n$ clusters via monolayer stacking. The sheet-like $Mg_nO_{2n}H_{2n}$ structures were predicted as the favored products of $(MgO)_n + nH_2O$, whereas more compact structures were found to dominate for the products of $(MgO)_n + mH_2O$, $m < n$. The stepwise hydrolysis reactions follow the compact reaction path until the crossover point is reached. Multi-step structural rearrangements are required for the conversion between the compact products and the sheet-like products even after the crossover point. The protective shell formed by the hydroxyl groups may inhibit the further hydrolysis reaction of the compact products, even though the hydrolysis reactions are exergonic. Plots of the normalized clustering energy vs. $n^{-1/3}$ give a linear fit and the $n = \infty$ value corresponds to the heat of fusion of the bulk. The agreement of the $n = \infty$ value with a combination of experiment for the bulk and Feller-Peterson-Dixon (FPD) heats of formation for the gas phase monomer is quite goodfro these systems. This approach can be used to estimate the heat of formation of the bulk mineral to provide bounds on these values and to check the consistency of calculations of the bulk thermodynamics. The results provide insights into the structural and energetic transitions from nanoclusters to the bulk. Models have been developed for the growth energetics to estimate the properties of larger clusters and the effects of solvation. FPD monomer energetics have been predicted for important mineral precursors including those with heavy and radioactive elements.

This work is part of the PNNL FWP 56674, "Molecular Mechanisms of Interfacial Reactivity in Near Surface and Extreme Geochemical Environments".

Postdoctoral Fellows: K. Sahan Thanthiriwatte, Monica Vasiliu

Publications

Chen, M.; Felmy, A.R.; Dixon, D.A. Structures and Stabilities of $(MgO)_n$ Nanoclusters. J. *Phys. Chem. A* **2014**, *118*, 3136–3146. DOI: 10.1021/jp412820z

Jackson, V.E.; Felmy, A.R.; Dixon, D.A. The Prediction of the pK_as of Aqueous Metal Ion Complexes. *J. Phys. Chem. A* **2015**, *119*, 2926-2939, DOI: 10.1021/jp5118272.

Chen, M.; Jackson, V.E.; Felmy, A.R.; Dixon, D.A. Structures and Stabilities of $(MgCO_3)_n$ Clusters, $n \leq 16$. *J. Phys. Chem. A* **2015**, *119*, 3419–3428. DOI: 10.1021/jp511823k

Qafoku, O.; Dixon, D.A.; Rosso, K.M.; Arey, B.W.; Felmy, A.R. Dynamics of Magnesite Formation at Low-Temperature and High-pCO_2 in Aqueous Solution. *Environ. Sci. Technol.* **2015**, *49*, 10736–10744. DOI: 10.1021/acs.est.5b02588

Finney, B.; Thanthirwatte, K.S.; Francisco, J.S.; Dixon, D.A. Energetic Properties and Electronic Structure of [C,N,O,P] and [C,N,S,P] Isomers. *J. Phys. Chem. A* **2017**, *121*, 2180-2186. DOI: 10.1021/acs.jpca.6b12673.

Dixon, D.A. Multiple contributions on electronic structure methods and elements in "Earth Sciences Series. Encyclopedia of Geochemistry," Ed. W. W. White, Section Ed. W. H. Casey, Springer International Publishing Switzerland 2017

Kelley, S. P.; Rogers, R. D.; Scott, B. L.; Runde, W. H.; Neu, M. P.; Dixon, D. A. Plutonium Coordination Chemistry in the Solid State. in Plutonium Handbook; 2nd ed.; Clark, D. L., Geeson, D. A., Hanrahan, R. J., Jr., Eds., 2017, Ch. 16. in press

NMR Spectroscopy on Aqueous Solutions to GPa Pressures

*Gerardo Ochoa[a], Matthew P. Augustine[a] and William H. Casey[a,b]**

[a]Department of Chemistry,
[b]Department of Earth and Planetary Sciences
University of California, Davis
1 Shields Ave, Davis, CA 95616 (USA);

Scope: We are developing a nuclear-magnetic resonance (NMR) probe that allows experiments on aqueous solutions to 2-4 GPa pressures and at ambient to hydrothermal conditions. It is so simple that undergraduate students can use it.

Objectives in this work are: **(1)** Measurements of aqueous speciation, and reaction dynamics, on aqueous molecules at pressures ranging from ambient to 3.0 GPa[1,2]. **(2)** Estimation of solute diffusion, and hence solution viscosities, *in situ*[3]. **(3)** Establishment of the normal array of two-dimensional NMR methods at extremely high pressures[4].

The design involves a clamp-cell and circuit coupled to a microcoil geometry and a fiberoptic cable coupled to a ruby sphere and laser in order to establish pressure (**Figure 1**, left). It is rigorously tested to 2.0 GPa[1-4], where spectra have been collected for nuclei such as ^{2}H, ^{1}H, ^{139}La, ^{11}B, ^{29}Si and ^{133}Cs, including conditions that are well beyond the nominal freezing pressure of solution to Ice VI (near 0.9 GPa). Freezing to form Ice VI is kinetically slow (minutes to hours) and electrolyte concentrations sharply increase the freezing pressure, so much so that solution NMR spectra can be collected to pressures that are nearly twice the nominal freezing pressure of H_2O. We also can employ pulsed-magnetic-field-gradient methods to collect two-dimensional NMR data and to measure the self-diffusion coefficient of H_2O in solutions[3]. The diffusion coefficients yield estimates of solution viscosity via the Stokes-Einstein relation and increased viscosity accounts for the pressure variation of T_1 values for simple electrolytes. Rates of molecular tumbling are slowed considerably by pressures in this range. Accounting for such changes is essential if NMR spectral line widths are used to infer pressure-enhanced rates of geochemical reactions.

Results during the last year include development of two-dimensional NMR methods[4] for liquids at GPa pressures (**Figure 2**). The figure shows ^{1}H-^{1}H correlation spectra for ethanol in a deuterated methanol solution to 2.8 GPa. The probe design is now being adapted to reach 3.0 or 3.5 GPa pressures by designing an *in situ* method of heating, which is essential to prevent freezing of aqueous solutions and extends the capabilities to geochemical conditions. We acquired a rod of the exotic NiCrAl alloy 40HNU-VI, largely unavailable in either Europe or the

U.S., through the assistance of Justin Carmichael[5] of Fermilab and Dr. Larry Anovitz of ORNL. This alloy is completely nonmagnetic and has exceptional strength[5-7]. The ultimate yield strength at ambient temperatures is 2.0-2.2 GPa. By comparison, Berylco-25, the standard material for high-pressure NMR probes, has an ultimate yield strength of 1.1 GPa and diminishes quickly with temperature so that it cannot be used much beyond ambient conditions. Acquisition of this 40HNU-VI alloy is particularly important because it retains a yield strength of 1.7 GPa at 500°C and should allow us to reach 3.5-4.0 GPa.

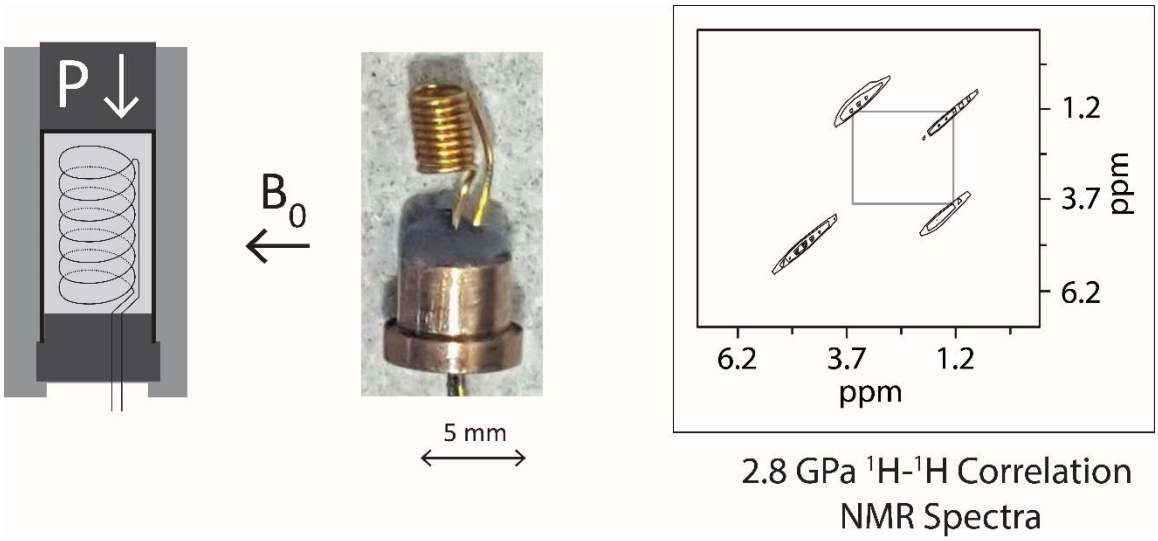

Figure 2: We collected ^{1}H-^{1}H chemical-shift correlation spectra (right) for a 1:4 ethyl:methyl alcohol mixture at 2.8 GPa. This mixture was chosen because it does not freeze at such high pressures. To collect high-resolution ^{1}H-NMR spectra, we use a magnet with the static magnetic field perpendicular to the bore, which allows us to rotate the solenoid to be coaxial (right and center). To our knowledge these are the highest-pressure chemical-shift-resolved NMR spectra measured.

Benefits to geochemistry and chemistry are profound. For geochemistry, this probe can directly detect solution speciation at pressures corresponding to well below the bottom of the Earth's crust, and perhaps hydrothermal temperatures. Geochemical models extend to such conditions but are now difficult to test[8-9]. Implications for broader chemistry and materials science are compelling--increasing pressure at ambient temperatures causes the dielectric constant of water to increase from 78 at to beyond 100. Electrostriction volumes become a large contribution to equilibrium reaction energies so that weak acids become strong acids and solvation drives processes that are impossible at ambient conditions. Equilibrium constants change by many orders of magnitude.

References Cited

1. Pautler, B.G., et al., A high-pressure NMR probe for aqueous geochemistry. *Angewandte Chemie International Edition*, 2014. **53**: p. 9788-9791.
2. Ochoa, G., et al., ^{2}H and ^{139}La NMR spectroscopy in aqueous solutions at geochemical pressures. *Angewandte Chemie International Edition,* 2015. **54**: p. 15444 –15447.
3. Ochoa, G., Augustine, M. A. and Casey, W. H. Nuclear magnetic resonance spectra of some electrolyte solutions to 1.9 GPa. 2016, *Geochim. Cosmochim. Acta* **193**, 66-74.
4. Augustine, M. P., Ochoa, G., and Casey, W. H. Steps to achieving high-resolution NMR spectroscopy on solutions at GPa pressure. 2017 *Am. J. Sci.* (in press).
5. Carmichael, J.R., *A high pressure cell for spark plasma sintering, a MSc thesis*, in *Materials Science and Engineering*. 2015, University of Tennessee, 2015. p. 54.
6. Walker, I.R., Considerations on the selection of alloys for use in pressure cells at low temperatures. *Cryogenics,* 2005. **45**(2): p. 87-108.
7. Walker, I.R., Nonmagnetic piston–cylinder pressure cell for use at 35 kbar and above. *Review of Scientific Instruments,* 1999. **70**(8): p. 3402-3412.
8. Sverjensky, D.A., B. Harrison, and D. Azzolini, Water in the deep Earth: The dielectric constant and the solubilities of quartz and corundum to 60 kbars and 1200°C. *Geochimica et Cosmochimica Acta,* 2014. **129**(0): p. 125-145.
9. Pan, D., et al., Dielectric properties of water under extreme conditions and transport of carbonates in the deep Earth. *Proceedings of the National Academy of Sciences,* 2013. **110**(17): p. 6646-6650.

New Light Shed on Important Earth-Relevant Redox Reactions Observed at the Nanoscale

Jie Xu[1], Mitsu Murayama[2], and Michael F. Hochella, Jr.[3,4]

[1] Department of Geological Sciences, the University of Texas at El Paso, El Paso, TX 79968
[2] Department of Materials Science and Engineering, Virginia Tech, Blacksburg, VA 24061
[3] Department of Geosciences, and NanoEarth, Virginia Tech, Blacksburg, VA 24061
[4] Geosciences Group, Pacific Northwest National Laboratory, 902 Battelle Blvd., Richland, WA 99354

The reduction-oxidation paired reaction is one of the foundational principles of chemistry. At first glance, redox chemistry is entirely straightforward, including at least the fundamental concepts of electron activities/redox potential (pE), the standard hydrogen electrode and Eh, and the Nernst equation. However, the reality of redox chemistry in complex systems, and particularly the most complex systems such as Earth, including biotic, abiotic, and mixed systems, can be exceptionally challenging to measure, understand, and anticipate or predict. Because much of the most important chemistry in nature is rooted in redox phenomena, and often critical to such fundamental processes as nucleation and precipitation, dissolution, ore deposits formation, contaminant generation and transport, and living system respiration and photosynthesis, just to name a few examples, it is assured that Earth systems redox chemistry will always be an essential topic of study and research. In this poster presentation, we will review a number of redox systems in nature that our group has looked at over the years, both abiotic and mixed abiotic/biotic, with most studied at the nanoscale which often sheds new light, and new discoveries, on these processes.

For example, we have examined the reduction of hematite nanoparticles of different sizes by *Shewanella oneidensis* MR-1, a dissimilatory iron reducing bacterium; the rate and extent of coupled reductive dissolution and Cr^{3+}_{aq} oxidation for seven Mn-oxides; and the low temperature nucleation and growth of Mn_3O_4 nanowires via the oxidation of aqueous Mn^{2+}_{aq} by dissolved oxygen in the presence of a nanocrystalline hematite catalyst. The latest redox effort from our group deals with our discovery of TiO_2 minerals naturally present in coal quickly converting to titania suboxides (Ti is partially reduced) during the coal's heating/burning in coal-fired power plants. This family of previously overlooked, incidental nano-materials is distributed via airborne and waterborne processes, likely globally. In its first toxicity testing, our work suggests that these unusual, widespread materials should be thoroughly tested for their toxicity in soils, sediments, and animals, and particularly in the human lung. We are also examining biogenic and abiogenic Fe-sulfide nanocrystals formed via the transformation of Fe(II) versus Fe(III) species. One of our hypotheses is that polysulfide phases can be formed through the shuttling of electrons from the aqueous sulfide to Fe(III). This work is highly relevant to the evolution of geochemical environments on both modern and ancient Earth.

Stern Layer Structure and Energetics at Mica-Water Interfaces

Ian Bourg, Princeton University

The screening of surface charge by dissolved ions at solid-liquid interfaces—in the region of interfacial fluid known as the electrical double layer (EDL)—plays a recurrent role in surface science, from ion adsorption to colloidal mechanics to the transport properties of nanoporous media. A persistent unknown in theories of EDL-related phenomena is the structure of the Stern layer, the near-surface portion of the EDL where water molecules and adsorbed ions form specific, short-range interactions with surface atoms. Here, we describe a set of synchrotron X-ray reflectivity (XRR) experiments and molecular dynamics (MD) simulations carried out in identical conditions, for a range of 0.1 M alkali chloride (Li-, Na-, K-, Rb-, or CsCl) solutions on the basal surface of muscovite mica, a mineral isostructural to phyllosilicate clay minerals and one of the most widely-studied reference surfaces in interfacial science. Our XRR and MD simulation results provide a remarkably consistent view of the structure and energetics of the Stern layer, with some discrepancy on the fraction of the minor outer-sphere component of Rb and on the adsorption energetics of Li. The results of both techniques, along with surface complexation model (SCM) calculations, provide insight into the sensitivity of water structure and ion adsorption to surface topography and the type of adsorbed counter-ion.

Simulation of fracture dissolution in rocks: a 3D approach

Vitaliy Starchenko, Larry Anovitz, Michael Cheshire, and Tony Ladd

The majority of the subsurface solute transport occurs in fractures. Understanding how to model fracture dissolution in rocks accurately will allow predicting the changes in fracture topology, channel formation, and can help to explain the early stages of cave formation and estimate the stability of underground storages and dams.

Typically, numerical models of fracture dissolution are simplified and represented by the system of one or two-dimensional fields. These approaches can explain many observations in nature such as wormhole formation (highly localized flow paths). However, such modeling is limited to the early stages of fracture dissolution where the variations in aperture are small. As the dissolution patterns develop, a 2D model is unable to correctly capture the flow in the vicinity of the wormholes and tends to overestimate the degree of competition between adjacent flow paths [*Starchenko et al.*, 2016].

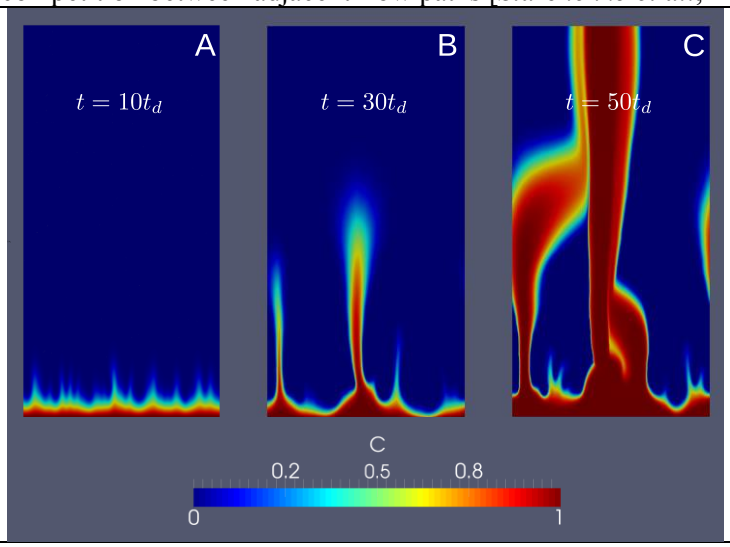

Fig.1. Distribution of the reactant concentration inside dissolved fracture. The slice is taken at the middle of the fracture, the plane is parallel to the fracture surface. Dissolution time: A – $10t_d$; B – $30t_d$; C – $50t_d$; where t_d is a time unit.

We have developed a three-dimensional numerical model that correctly captures the flow and reactant transport. Using this model, we have found that elliptically shaped channels can develop very early on, even before breakthrough, when the aperture h is in the millimeter range and the flow is still at low Reynolds number ($Re = uh/\nu \ll 1$, where ν is the kinematic fluid viscosity; which means fluid velocity u is small and the flow is laminar). There are qualitative differences in the aperture evolution after breakthrough, depending on whether the flow rate was limited externally or by the viscous drag on the fracture surfaces. At constant pressure drop after breakthrough the fracture tends to dissolve uniformly across its whole width. In case of limited flow rate well-developed conduits have been observed.

When the flow rate is low, almost all reactant is consumed within the dominant conduit, which enlarges without affecting the surrounding fracture matrix. At higher flow rates the consumption of reactant in the conduit becomes limited by the surface reaction rate while the remaining reactant dissolves the surrounding matrix. Therefore, using this model we can determine the condition when the wormhole formation becomes dominant and when rock dissolves uniformly. Moreover, in the case of limited flow after breakthrough bending of shorter channels toward the dominant one has been observed (Fig.1). This can explain such geological formations like anastomoses.

Lastly, we discuss the potential usage of the model for simulation of mineral dissolution in microfluidic devices on laboratory scale.

V. Starchenko, C. J. Marra, and A. J. C. Ladd (2016), Three-dimensional simulations of fracture dissolution, *J. Geophys. Res. Solid Earth*, *121*(9), 6421–6444, doi:10.1002/2016JB013321.

Adsorption of Copper and Iron on Mesoporous Alumina and Silica

A. Knight, A. Tigges, R. Washington, and A. Ilgen

Geochemistry Department, Sandia National Laboratories, Albuquerque, New Mexico 87185

Recent studies in geochemistry have observed that material properties such as fluid viscosity, ion transport, and interfacial chemistry are dependent on pore-size. Nano-confinement impacts heterogeneous adsorption and redox reactions that control the fate and transport of chemical species in soils, sediments, and consolidated porous rocks. The presence of nano-scale confined domains in tight rocks (e.g., shale) has been recognized as the main factor affecting the selective permeability of these rocks. Thermodynamic equilibrium between solids and fluids in small pores (< 100 nm) differs from the equilibrium observed between a solid surface in contact with a bulk fluid. This difference is due to the relatively large ratio of mineral-surface-bound (structured) water molecules in nano-scale confined systems, compared to in bulk water. This leads to a decrease in the dielectric constant (for pores < 5nm) and density of water, causing a decrease in the solvation energy of metal cations.[1-3] Because of the decreased solvation energy of metal cations, enhanced inner-sphere complexation is observed and adsorption onto mineral surfaces is promoted.[3-4]

The goal of our project is to systematically evaluate the effects of nano-scale confinement on the adsorption properties of copper (Cu^{2+}) and iron ($Fe^{2+/3+}$) on mesoporous silica and alumina. These materials are ideal substrates for this study because silanol and aluminol functional groups are surface sites common to many minerals and because these materials have a narrow pore size distribution (2 nm to 8 nm) that includes sizes where nano-scale confinement effects are observed.

In this study we analyzed the adsorption of Cu^{2+} and $Fe^{2+/3+}$ to obtain the thermodynamic and kinetics parameters that govern the adsorption process, and compared the surface-area normalized adsorption of silica and alumina as the pore size decreased. For silica (4 – 8 nm), we saw no significant difference between the surface-area normalized adsorption of Cu^{2+} with pore sizes 6 nm and 8 nm. However, when the pore size is 4 nm, we observed an enhancement in the Cu^{2+} adsorption, and a nearly 5-fold increase in the adsorption capacity when fit with a Fruendlich isotherm. This result is consistent with the effects of nano-scale confinement, where a decrease in the hydration energies of metals, as the pore size decreases below 5 nm, has demonstrated enhanced adsorption properties.[3-5] Furthermore, the adsorption kinetics show a pseudo-first order kinetic rate for Cu^{2+} on both silica and alumina, where the rate constants, k, are higher for silica than alumina. This agrees with the expected adsorption pathway in which surface adsorption on alumina favors inner-sphere complexation while silica favors outer-sphere. Preliminary data investigating the adsorption of $Fe^{2+/3+}$ suggest nano-scale confinement effects are observed; more ongoing experiments are being performed to further quantify the impact of nano-scale confinement.

Future experiments will aim to understand the coordination environment of the adsorbed species of Cu and Fe. We will analyze the solid materials post adsorption at the Advanced Photon Source by X-ray absorption spectroscopy (XAFS and XANES). We hypothesize that there will be marked changes in the bond distances of the central metal to nearest oxygen neighbors resulting from nano-scale confinement.

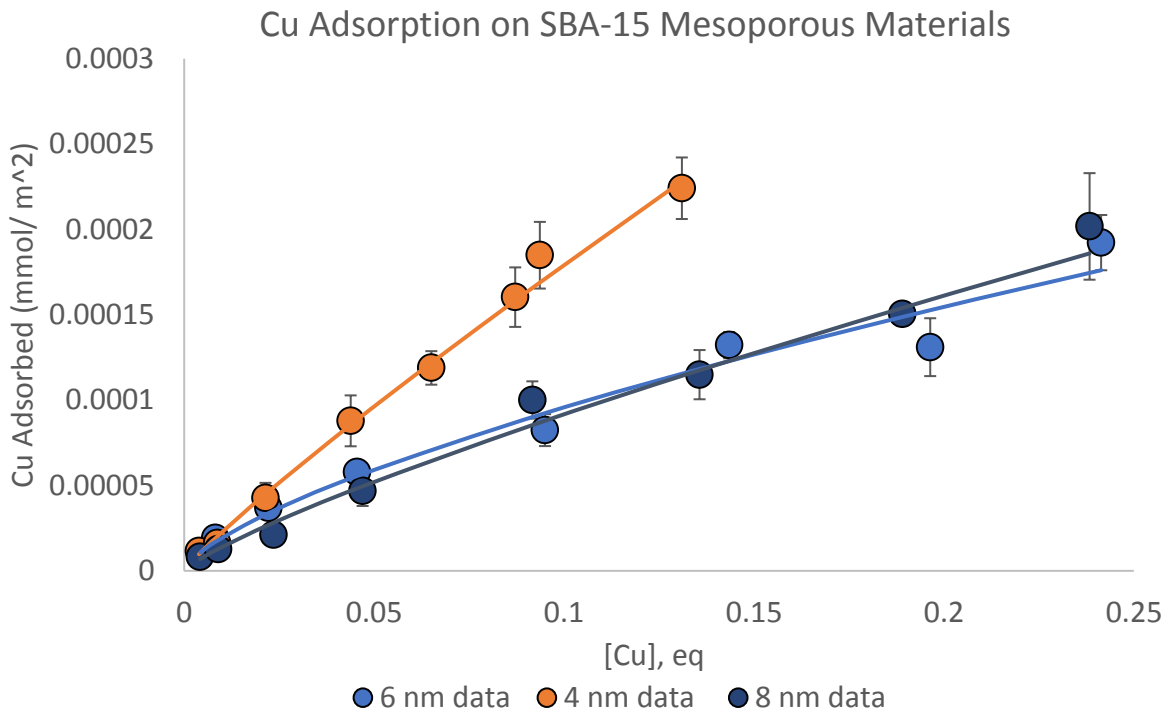

Figure 1. Surface area normalized adsorption of Cu on mesoporous silica (4, 6, and 8 nm) fit with Fruendlich isotherm. These data highlight the enhanced adsorption of Cu when the pore volume decreases to a 4 nm pore.

Sandia National Laboratories is a multimission laboratory managed and operated by National Technology and Engineering Solutions of Sandia LLC, a wholly owned subsidiary of Honeywell International Inc. for the U.S. Department of Energy's National Nuclear Security Administration under contract DE-NA0003525.

[1] Marti, J.; Nagy, G.; Guardia, E.; Gordillo, M. C. Molecular dynamics simulation of liquid water confined inside graphite channels: Dielectric and dynamical properties. *J. Phys. Chem. B* **2006,** *110* (47), 23987-23994.

[2] Takei, T.; Mukasa, K.; Kofuji, M.; Fuji, M.; Watanabe, T.; Chikazawa, M.; Kanazawa, T. Changes in density and surface tension of water in silica pores. *Colloid Polym. Sci.* **2000,** *278* (5), 475-480.

[3] Wang, Y. F.; Bryan, C.; Xu, H. F.; Gao, H. Z. Surface chemistry of mesoporous materials: Effect of nanopore confinement. *Mater. Res. Soc. Symp. P.* **2003,** *751*, 121-125.

[4] Kalluri, R. K.; Konatham, D.; Striolo, A. Aqueous NaCl Solutions within Charged Carbon-Slit Pores: Partition Coefficients and Density Distributions from Molecular Dynamics Simulations. *J. Phys. Chem. C* **2011,** *115* (28), 13786-13795.

[5] Nelson, J. M.; Bargar, J. R.; Brown, G. E.; Maher, K. Probing the mechanisms of pore size dependent geochemistry: Effects of meso-confinement on Zn sorption in mesoporous silica. *Abstr. Pap. Am. Chem. S.* **2014,** *247*.

Geophysical Methods for Geochemical and Hydrological Processes at Mineral-water Interfaces of Geological Media

Yuxin Wu, Lawrence Berkeley National laboratory

Geochemical processes at mineral-water interfaces, such as dissolution and precipitation, play a key role in controlling the evolution of the physical and hydrological properties of geological media. Understanding how interfacial geochemical processes manifest at larger continuum scales with a collective impact on rock mechanical or flow properties require the joint used of both geophysical and geochemical approach. A key component of the approach is to identify and understand a set of geophysical signals that are sensitive to geochemical processes at mineral-water interfaces but are manifested at large, continuum scales.

Electrical geophysical methods have proven sensitivity to the interfacial geochemical processes that lead to physiochemical transformations of rocks and fluids at larger scales. We present our study on interfacial complex charge conduction and polarization behavior measured with geophysical methods at centimeter and larger scales, and how they are linked with the hydrological and geochemical properties and processes at mineral-water interfaces. Specifically, we demonstrate (1) the sensitivity of complex interfacial conductivity signal to mineral precipitates, such as calcite and iron oxides; (2) the impacts of pore water chemistry, such as pH and saturation, on the complex electrical signals; (3) the development of novel geophysical contrasting agents that can be used to illuminate preferential flow paths in fracture rocks; and (4) how geophysical methods can be used to monitor hydrological property changes during geochemical transformations.